

Table 1 Clinical characteristics of 76 neuroblastomas detected by MS in one institution

Clinical characteristics		No. of patients
Stage	stage 1, 2, 4S	65 (86%)
	stage 3, 4	11
Primary site	not adrenal	34 (45%)
	adrenal	42
Operation	complete resection	53
	incomplete resection	23
Chemotherapy	not done	19
	done	57
Outcome	alive	74
	dead	2

Table 2 Biological prognostic factors of 76 MS cases

Biological prognostic factors		No. of patients
MYCN amplification	not amp.	69
	amp.	5 (7%)
1p deletion	no deletion	22
	deletion	2 (8%)
17q gain	no gain	30
	gain	3 (9%)
TrkA expression	high expression	24
	low expression	1 (4%)
DNA ploidy	aneuploid	45
	diploid	5 (10%)
Shimada histology	favorable	74
	unfavorable	2 (3%)

Table 3 Clinical features of 13 cases with unfavorable factors

Case no.	Number of positive unfavorable factors	Stage (INSS)	Initial operation of primary tumor	Initial chemotherapy	Recurrence	Outcome
1	1	3	incomplete resection	multi-drug	-	CR
2	1	1	complete resection	mild	-	CR
3	2	3	incomplete resection	mild	-	CR
4	1	1	complete resection	mild	-	CR
5	1	3	incomplete resection	mild	-	CR
6	1	1	complete resection	-	-	CR
7	1	1	complete resection	mild	-	CR
8	3	1	complete resection	-	+	2nd CR
9	3	4S	complete resection	mild, multi-drug	-	*RT
10	1	1	complete resection	-	-	CR
11	1	2A	incomplete resection	mild	-	CR
12	1	1	complete resection	-	-	CR
13	1	1	complete resection	-	+	CR → PD

CR: complete response; PD: progressive disease; *RT: residual tumor of liver metastasis

stage 1 while the third case was stage 2A. Two cases underwent complete resection of the primary tumor, and 1 case had an incomplete resection of the tumor. Regarding the initial chemotherapy, 1 case received mild chemotherapy (a low dose of CPA and VCR), while 2 cases received no chemotherapy. The time from initial therapy to relapse ranged from 7 months to 48 months. The patterns of relapse included one local relapse, 1 metastatic recurrence, and 1 local and metastatic recurrence. Regarding the treatment for relapse, 2 patients (cases 14 and 15) underwent partial resection for local recurrences, and all 3 cases received high dose multi-drug chemotherapy such as the A1 protocol without peripheral blood stem cell transplantation. Regarding the outcome after relapse, 2 cases demonstrated a 2nd CR, 1 case has multiple progressive tumors.

Two patients of the 76 patients have shown refractory disease. Their clinical courses are shown in Table 5. Case 9 was diagnosed at 6 months of age to be right adrenal neuroblastoma with multi-

ple liver metastatic lesions. Mild chemotherapy (a low dose of CPA and VCR) was administered after a complete resection of the primary tumor. However, the size and number of the multiple liver metastases did not change. As a result, intensive multiple drug chemotherapy (CPA, VCR, THP-ADR, CDDP) was started. After 3 courses of intensive chemotherapy, a liver biopsy was performed due to the fact that no change in the size of the liver metastases was observed. A number of viable ganglioneuroblast cells were present in the liver biopsy sample, which was similar to the findings in the liver metastasis at the primary operation. As a result, more intensive chemotherapy (CPA, VP-16, THP-ADR, CDDP) was administered after performing a liver biopsy. Thus, intensive chemotherapy was continued for 15 months. The patient has remained alive for 6 years since the initial diagnosis without any change in the size and number of liver metastases. Case 16 was diagnosed at 6 months of age as having a stage 3 retroperitoneal neuroblastoma involving the celiac artery. The patient was observed for 6 months without any surgical interven-

Table 4 Recurring neuroblastomas in 76 MS cases

Case no.	Stage	Initial operation chemotherapy	Time from initial therapy to recurrence	Pattern of recurrence treatment for recurrence	Outcome
8	1 (C1N0B0V0bm0H0D0)	complete resection (-)	21 months	bone and bone marrow New A1 → CPA, THP-ADR	2nd CR
14	1 (C1N0B0V0bm0H0D0)	complete resection (-)	7 months	local recurrence, lung, liver partial resection → A1	PD
15	2A (C3N0B0V0bm0H0D0)	partial resection mild (1 year)	48 months	local recurrence partial resection → A1	2nd CR

Mild: low dose of CPA and VCR; New A1: CPA, VP-16, THP-ADR, CDDP; A1: CPA, VCR, THP-ADR, CDDP; CR: complete response; PD: progressive disease

Table 5 Refractory neuroblastomas in 76 MS cases

Case no.	Stage	Initial operation of primary tumor	Chemotherapy	Time from initial therapy	Outcome
9	4S (C1N0B0V0bm0H1D0)	complete resection	mild → new A1 → C and A2 (30 months)	7 years	residual multiple liver metastasis
16	3 (C3N0B0V0bm0H0D0)	biopsy	mild (1 year)	6 years	residual local tumor (size: no change)

New A1: CPA, VP-16, THP-ADR, CDDP; C and A2: CPA, DTIC and CPA, VCR, THP-ADR, CDDP; Mild: low dose of CPA and VCR

Table 6 Prognostic factors of recurrent or refractory neuroblastomas

Case	MYCN amp.	1p deletion	DNA ploidy	TrkA expression	Shimada	17q gain
8	-	-	diploid	low	favorable	+
14	-	-	diploid	high	favorable	-
15	-	-	aneuploid	high	favorable	-
9	6 copies	+	diploid	high	favorable	-
16	-	-	aneuploid	high	favorable	-

tion according to the parents' wish because complete resection of the retroperitoneal mass was deemed to be impossible. However, the level of urinary VMA and HVA increased gradually, and therefore an open biopsy of the primary tumor was performed at 6 months after the initial diagnosis. Mild chemotherapy (a low dose of CPA and VCR) was administered for 1 year after the open biopsy of the primary tumor. However, the size of the tumor and the level of urinary VMA and HVA did not change. The patient has remained alive for 6 years since the initial diagnosis with no change in the size of the tumors and a slight decrease in the level of urinary VMA and HVA.

Table 6 shows the prognostic factors for the primary tumor in recurrent or refractory neuroblastomas. Three cases had one or more unfavorable factors, while 2 cases had no unfavorable factors. Only one case (case 9) showed MYCN amplification (6 copies). In cases 14 and 15, the biological findings of recurrent tumors corresponded to the findings of the primary tumor.

Discussion

We have previously reported that the majority of neuroblastoma detected by MS have a good prognosis, while a few cases have an unfavorable outcome. The purpose of MS at 6 months of age was to decrease the number of advanced-stage neuroblastoma patients over 1 year of age and reduce the mortality due to neuroblastoma. Regrettably, this purpose was not achieved [8,17]. However, we have obtained different insights into infantile neuroblastoma based on the clinical and biological features of neuroblastoma detected through MS at 6 months of age in Japan.

In the present study, the clinical characteristics of the 76 MS cases at our institution were almost the same as these reported by others [2,13]. However, detailed reports on the clinical features of MS cases with biologically unfavorable factors and the biological features of recurrent or refractory MS cases are rare. A total of 13 of the 76 MS cases presented with one or more biologically unfavorable factors. Our result demonstrates that at least 17% of the neuroblastomas detected by MS have biologically unfavorable factors. The frequency (23%) of recurrent or refractory

Original article
 Accepted for publication: 15.08.2006
 15

cases (3 patients) in the 13 cases with biologically unfavorable factors was significantly higher than that (3%) of recurrent or refractory cases (2 patients) in the 63 cases without any biologically unfavorable factors ($p < 0.05$, Fisher's exact test). Furthermore, 2 out of 3 cases with multiple unfavorable factors presented with recurrent or refractory disease. Of the 5 recurrent or refractory cases, 3 cases had one or more biologically unfavorable factors, while 2 cases had no biologically unfavorable factors. This finding suggests that biologically unfavorable factors are associated with a high risk of recurrence in infantile neuroblastomas. Regarding the *MYCN* amplification status in the 5 recurrent or refractory cases, only one case revealed *MYCN* amplification using the Southern Blot method, FISH method and the quantitative PCR method. Two of the recurrent or refractory cases had other unfavorable factors than *MYCN* amplification. In many previous reports on infantile neuroblastomas, the real outcome of neuroblastoma with other prognostic factors than *MYCN* amplification was unclear. Our study suggests that some of these tumors may progress and eventually some patients may die, if they are not detected during mass screening at 6 months of age and, as a result, do not undergo any immediate surgical intervention with or without additional treatment. The immediate surgical intervention with or without additional treatment is therefore essential and should be beneficial for such patient groups. It may therefore be important to analyze other prognostic factors than just the *MYCN* amplification status in infantile neuroblastoma cases. On the other hand, 2 recurrent or refractory cases had no unfavorable factors, and the reason for this remains unclear. A prospective evaluation of these factors in larger patient cohorts is required to establish their prognostic significance.

Recent reports describe the clinical course of MS cases managed with non-treatment and observation (non-surgical intervention and no chemotherapy) [4,18]. The Committee for the Japanese Association of Pediatric Oncology analyzed 82 MS cases at 17 institutions managed by non-treatment and observation in 1998 [11]. Of these 82 cases, 22 subsequently underwent surgical intervention because of an increased tumor size, either with or without an increase in the urinary VMA and HVA levels ($n = 15$) or at the parents' request ($n = 7$). Of the 60 cases initially observed without surgical intervention, tumors disappeared in only 17 cases while they persisted in 43. All 82 patients in the cohort are still alive. However, the clinical course of the non-treatment cases may not be representative of the natural course of infantile neuroblastomas because the non-treatment cases included few patients with stage 1 or 2 disease associated with relatively low levels of urinary VMA and HVA, and had no invasion into the surrounding organs and vessels. Therefore, these findings do not support management by non-treatment and observation for infantile neuroblastomas. Instead, biological factors appear best able to predict whether an infantile neuroblastoma will regress spontaneously or grow aggressively.

In conclusion, regarding the neuroblastoma detected by MS at one institution in Japan, 17% had one or more biologically unfavorable factors and might thus have a higher risk of recurrence than the patients without such biologically unfavorable factors, although the unfavorable biology of several refractory cases re-

mains unclear, even after performing highly sensitive analysis. At least one-fifth of the neuroblastomas detected by MS are anticipated cases. In infantile neuroblastomas, the most important action may be to biologically analyze the prognostic factors using highly sensitive methods after performing immediate surgical intervention. Since the MS program has been discontinued in Japan, it will be necessary in future to assess the mortality and the characteristics of neuroblastoma detected clinically.

References

- 1 Bessho F, Hashizume K, Nakajo T et al. Mass screening in Japan increased the detection of infants with neuroblastoma without a decrease in cases in older children. *J Pediatr* 1991; 119: 237–241
- 2 Hachitanda Y, Ishimoto K, Hata J, Shimada H. One hundred neuroblastoma detected through a mass screening system in Japan. *Cancer* 1994; 74: 3223–3226
- 3 Matsumura T, Shikata T, Sawada T. Treatment modality for neuroblastoma infants in Japan: Retrospective analysis and future directions. Proceeding of the 31st American Society of Clinical Oncology. *J Clin Oncol* 1995; 14: 456
- 4 Oue T, Inoue M, Yoneda A et al. Profile of neuroblastoma detected by mass screening resected after observation without treatment: results of the wait and see pilot study. *J Pediatr Surg* 2005; 40: 359–363
- 5 Sawada T, Kidowaki T, Sakamoto I et al. Neuroblastoma: Mass screening for early detection and its prognosis. *Cancer* 1984; 53: 2731–2735
- 6 Shimada H, Chatten J, Newton Jr WA, Sachs N, Hamoudi AB, Chiba T et al. Histopathologic prognostic factors in neuroblastic tumors: definition of subtypes of ganglioneuroblastoma and an age-linked classification of neuroblastomas. *J Natl Cancer Inst* 1984; 73: 405–416
- 7 Suita S, Zaizen Y, Sera Y et al. Mass screening for neuroblastoma: quo vadis? A 9-year experience from the Pediatric Oncology Study Group of the Kyushu area in Japan. *J Pediatr Surg* 1996; 31: 555–558
- 8 Suita S, Tajiri T, Akazawa K, Sera Y, Takamatsu H, Mizote H, et al. Mass screening for neuroblastoma at 6 months of age: difficult to justify. *J Pediatr Surg* 1998; 33: 1674–1678
- 9 Suita S. Mass screening for neuroblastoma in Japan: lessons learned and future directions. *J Pediatr Surg* 2002; 37: 949–954
- 10 Suita S, Zaizen Y, Yano H, Akiyama H, Sera Y, Takamatsu H et al. How to deal with advanced cases of neuroblastoma detected by mass screening: a report from the Pediatric Oncology Study Group of the Kyushu area of Japan. *J Pediatr Surg* 1994; 29: 599–603
- 11 Suita S, Sawada T, Kaneko M, Tajiri T, Naito M, Hayashi Y et al. The report of the committee for neuroblastoma at the Japanese association of Pediatric Oncology at 1998. *Jpn J Pediatr Oncol* 1999; 36: 107–117
- 12 Tanaka S, Tajiri T, Suita S et al. Clinical significance of a highly sensitive analysis for gene dosage and the expression level of *MYCN* in neuroblastoma. *J Pediatr Surg* 2004; 39: 63–68
- 13 Tanaka T, Sugimoto T, Sawada T. Prognostic discrimination among neuroblastomas according to Ha-ras/Trk A gene expression: a comparison of the profiles of neuroblastomas detected clinically and those detected through mass screening. *Cancer* 1998; 83: 1626–1633
- 14 Tajiri T, Shono K, Tanaka S et al. Evaluation of genetic heterogeneity in neuroblastoma. *Surgery* 2002; 131: 283–287
- 15 Tajiri T, Tanaka S, Shono K et al. Quick quantitative analysis of gene dosages associated with prognosis in neuroblastoma. *Cancer Lett* 2001; 166: 89–94
- 16 Tajiri T, Suita S, Takamatsu H, et al. Clinical and biologic characteristics for recurring neuroblastoma at mass screening cases in Japan. *Cancer* 2001; 15: 349–353
- 17 Yamamoto K, Ohata S, Ito E et al. Marginal decrease in mortality and marked increase in incidence as a result of neuroblastoma screening at 6 months of age: cohort study in seven prefectures in Japan. *J Clin Oncol* 2002; 20: 1209–1214
- 18 Yamamoto K, Hanada R, Tanimura M, Aihara T, Hayashi Y. Natural history of neuroblastoma found by mass screening. *Lancet* 1997; 349: 1102

High expression of *N*-acetylglucosaminyltransferase V in favorable neuroblastomas: Involvement of its effect on apoptosis

Kei-ichiro Inamori^a, Jianguo Gu^{a,*}, Miki Ohira^b, Atsushi Kawasaki^b, Yohko Nakamura^b, Takatoshi Nakagawa^c, Akihiro Kondo^c, Eiji Miyoshi^a, Akira Nakagawara^b, Naoyuki Taniguchi^a

^a Department of Biochemistry, Osaka University Graduate School of Medicine, 2-2 Yamadaoka, Suita, Osaka 565-0871, Japan

^b Division of Biochemistry, Chiba Cancer Center Research Institute, 666-2 Nitona, Chuoh-ku, Chiba 260-8717, Japan

^c Department of Glycotherapeutics, Osaka University Graduate School of Medicine, 2-2 Yamadaoka, Suita, Osaka 565-0871, Japan

Received 1 December 2005; revised 27 December 2005; accepted 29 December 2005

Available online 5 January 2006

Edited by Laszlo Nagy

Abstract Neuroblastoma (NBL), derived from the sympathetic precursor cells, is one of the most common pediatric solid tumors. The expression of *N*-acetylglucosaminyltransferase V and IX (GnT-V and GnT-IX) mRNA in 126 primary NBLs were quantitatively analyzed and higher expression levels of GnT-V were found to be associated with favorable stages (1, 2 and 4s). Conversely, the downregulation of GnT-V expression by small interfering RNA resulted in a decrease in the susceptibility to cell apoptosis induced by retinoic acid in NBL cells accompanied by morphological change. These results suggest that GnT-V is associated with prognosis by modulating the sensitivity of NBLs to apoptosis.

© 2006 Federation of European Biochemical Societies. Published by Elsevier B.V. All rights reserved.

Keywords: Neuroblastoma; GnT-V; GnT-IX; Retinoic acid; Apoptosis

1. Introduction

Aberrant glycosylation occurs in nearly all types of cancers, and has been implicated in the malignancy that is characteristic of the disease [1]. *N*-acetylglucosaminyltransferase V (GnT-V) is one of the most relevant glycosyltransferases to tumor invasion and metastasis, and catalyzes the formation of β 1,6GlcNAc branching on *N*-glycans, which is closely associated with malignant transformations [2–6]. Recently, our group and Pierce's group independently reported on a new *N*-acetylglucosaminyltransferase IX (GnT-IX, also referred to as GnT-VB), a GnT-V homolog, that is specifically expressed in the brain [7,8]. GnT-IX transcripts are exclusively expressed in the brain and testis, while GnT-V is expressed ubiquitously in human and mouse tissues. Since both glycosyltransferases are expressed in the mouse brain in a region-specific manner (unpublished data), it is possible that they may have discrete biological functions in the brain. On the other hand, GnT-V and GnT-IX are both highly expressed in both the adult and

fetal brain [7,9], as well as in several human neuroblastoma (NBL) cell lines (this study and unpublished data). This prompted us to examine the expression of GnT-V and GnT-IX in primary NBL tissues.

NBL is a tumor derived from primitive cells of the sympathetic nervous system and is the most common solid tumor in childhood [10]. Interestingly, most NBLs in infants regress spontaneously or mature into a benign ganglioneuroma. These tumors usually express high levels of TrkA, and as a result, have a tendency to either undergo apoptosis or differentiation, depending on whether nerve growth factor is present or absent in their microenvironment. On the other hand, in most patients over 1 year of age who have metastatic disease, the tumor grows aggressively and their prognosis is usually poor.

In this study, we carried out a quantitative analysis of the gene expression of these glycosyltransferases by real-time PCR, and the findings indicate that a higher expression of GnT-V is correlated with a favorable prognosis for NBL patients. Furthermore, to explore the underlying molecular mechanism, we devised a knockdown approach, in which small interfering RNA (siRNA)-directed against GnT-V mRNA was used to investigate the susceptibility to cell apoptosis induced by retinoic acid in NBL cells. The results clearly showed that the expression levels of GnT-V are associated with a favorable prognosis, possibly through sensitizing to apoptotic signals.

2. Materials and methods

2.1. RNA isolation from primary NBLs

Fresh, frozen tumor tissues were sent to the Division of Biochemistry, Chiba Cancer Center Research Institute, from various hospitals in Japan with informed consent from the patients' parents. All samples were obtained by surgery or biopsy and had been stored at 80 °C. The RNA samples obtained from 126 patients with NBL were subjected to semiquantitative and quantitative real-time reverse transcription-PCR (RT-PCR) analyses. All of the patients were diagnosed clinically as well as pathologically and were tested for DNA ploidy, MYCN amplification, and TrkA expression. The tumors were staged according to the criteria of the International Neuroblastoma Staging System [11].

2.2. Semiquantitative RT-PCR analysis of primary NBLs

The preparation of total RNA from NBL tissues and the synthesis of the first-strand cDNA were performed as described previously [12]. The cDNA was diluted to a 1:20 solution and then amplified in a final

*Corresponding author. Fax: +81 6 6879 3429.

E-mail address: jgu@biochem.med.osaka-u.ac.jp (J. Gu).

Abbreviations: NBL, neuroblastoma; GnT-V, *N*-acetylglucosaminyltransferase V; GnT-IX, *N*-acetylglucosaminyltransferase IX; RT, reverse transcription; PARP, poly(ADP-ribose) polymerase

volume of 10 μ l of reaction mixture containing 200 μ M of dNTPs, 1 \times PCR buffer, 0.5 μ M of each primer and 0.2 U of rTaq DNA polymerase (Takara Bio, Ohtsu, Japan). The following primer sets were used: GnT-V, 5'-GACCTGCAGTTCCTTCTTCG-3' and 5'-CCATGGCA-GAAGTCTGTTT-3'; GnT-IX, 5'-CATGGCACCGTGTACTAC-3' and 5'-TCTGGAGCTCTGCAGAAAG-3'. PCR templates were standardized by their GAPDH expression before performing the RT-PCR experiments.

2.3. Quantitative real-time PCR analysis of primary NBLs

2 μ l of cDNA prepared as above, either a 100-fold dilution for GnT-V or a 20-fold dilution for GnT-IX, was amplified in a volume of 20 μ l with Assay-on-Demand Gene Expression Products (Applied Biosystems) consisting of primers and a TaqMan probe (Assay ID: GnT-V, Hs00159136_m1; GnT-IX, Hs01586304_g1). The thermal cycling conditions and the normalization of the data using GAPDH expression were performed as described previously [12]. All experiments were carried out in triplicate for each data point.

2.4. Assay of GlcNAc transferase activity

The activities of GnT-V and GnT-III in whole cell lysates or microsomal fractions were determined using a pyridylaminated biannary sugar chain as an acceptor substrate, as described previously [7,13].

2.5. Construction of siRNA vector and retroviral infection

Small interfering oligonucleotides specific for GnT-V were designed on the Takara Bio website (<http://www.takara-bio.co.jp/>) and the oligonucleotide sequences used in the construction of the siRNA vector were as follows: 5'-GATCCGTTTCATTGGCGGAAATTCGTTTCAAGA-GAACGAATTTCCGCCAATGAACTTTTTTAT-3' and 5'-CGA-TAAAAAAGTTTCATTGGCGGAAATTCGTTTCTTTGAAACGA-ATTTCCGCCAATGAACG-3'. The oligonucleotides were annealed and then ligated into *Bam*HI/*Cla*I sites of the pSINsi-hU6 vector (Takara Bio). A retroviral supernatant was obtained by transfection of human embryonic kidney 293 cells using a Retrovirus Packaging Kit Amphi (Takara Bio) according to the manufacturer's protocol. CHP134 cells, a human NBL cell line, were infected with the viral supernatant, and the cells were then selected with 0.5 mg/ml G418 for 2–3 weeks. Stable GnT-V-knockdown clones were selected and confirmed by GnT-V activity and gene expression. Quantitative real-time PCR analyses of GnT-V mRNA expression in these clones were performed with a Smart Cycler II System and the SYBR premix Taq (Takara Bio). RT was carried out at 42 $^{\circ}$ C for 10 min, followed by 95 $^{\circ}$ C for 2 min using random primers, followed by PCR for 50 cycles at 95 $^{\circ}$ C for 5 s and 60 $^{\circ}$ C for 20 s with the following primers: 5'-AAG-CAGGTGTGCCAGGAGAG-3' and 5'-GTCAAAGGAGGGCAC-CAGGA-3'. Normalization of the data was performed using the GAPDH mRNA levels.

2.6. Analysis of retinoic acid-induced apoptosis

Parent, mock, and GnT-V-knockdown CHP134 cells were plated on 10 cm culture dishes at 5×10^5 cells in RPMI1640 supplemented with 10% fetal bovine serum, 100 U/ml penicillin, and 0.1 mg/ml streptomycin. After incubation for 24 h, the conditioned media were changed with fresh medium containing various concentrations of all-*trans* retinoic acid (Sigma). The cells were washed twice with PBS and harvested at the indicated times. Retinoic acid-induced apoptosis was estimated by detecting the cleavage of poly ADP-ribose polymerase (PARP) in whole cell lysates by Western blot analysis using a human specific anti-cleaved PARP (Asp214) antibody (Cell Signaling Technology). As a loading control, anti-ERK1/2 (p44/42 MAP Kinase Antibody, Cell Signaling Technology) was used.

2.7. Viability assay of retinoic acid-treated cells

The parent, mock, and GnT-V-knockdown CHP134 cells were seeded on a 96-well plate at 3×10^3 cells/well for 24 h prior to the retinoic acid treatment. The cells were then incubated with or without retinoic acid at the indicated concentrations for 3 days. Cell viability was assayed using a Cell Counting Kit-8 (Dojindo, Kumamoto, Japan) according to the manufacturer's instructions. All experiments were carried out in triplicate for each data point.

3. Results

3.1. Association between higher expression levels of GnT-V mRNA and favorable prognosis in primary NBLs

To assess the association between GnT-V or GnT-IX mRNA expression and the prognosis of the NBLs, we first performed semiquantitative RT-PCR analyses using 16 favorable and 16 unfavorable NBLs. As shown in Fig. 1, GnT-V was preferentially expressed in most of the favorable NBLs, while no obvious difference in GnT-IX expression was found between favorable and unfavorable NBLs. Table 1 shows quantitative data for GnT-V and GnT-IX mRNA in 126 primary NBLs with tumor stages (1, 2, 4s versus 3, 4). GnT-V expression was significantly increased in NBLs at favorable stages ($P = 0.021$), and was correlated well with higher expression of *TrkA* ($P = 0.010$). On the other hand, GnT-IX expression was marginally associated with the stages.

3.2. GnT-V activities in various human NBL cell lines

To determine whether the expression level of GnT-V is also increased in NBL cells, the activities of GnT-V in various human NBL cell lines were examined. As shown in Fig. 2A, each cell line expressed GnT-V activity at distinct levels. The CHP134 cells showed the highest GnT-V activity among the 10 NBL cell lines used in this study. It is known that the cell line is highly sensitive to the induction of apoptosis by all-*trans* retinoic acid [14,15]. In fact, it is thought that favorable NBLs usually express higher levels of *TrkA*, and tend to regress spontaneously due to apoptosis. As shown in Fig. 2B, in CHP134 cells that had been treated with retinoic acid at a concentration of 1 μ M or 5 μ M, PARP cleavage, a marker for apoptosis, occurred, which is one of the main cleavage targets of caspase-3

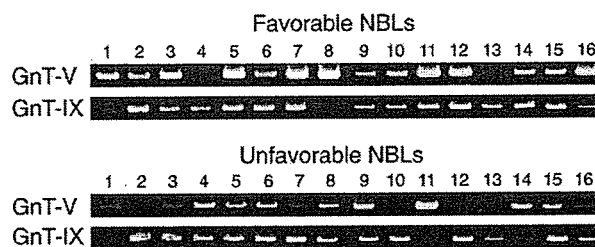


Fig. 1. Semiquantitative RT-PCR analysis of favorable and unfavorable subsets of NBL. Sixteen favorable cases were in stage 1 with no MYCN amplification and a high *TrkA* expression, while 16 unfavorable cases were in stage 3 or 4 with MYCN amplification and a low *TrkA* expression.

Table 1
Association of tumor stages and *TrkA* expression in NBL patients with GnT-V or GnT-IX mRNA expression levels

	<i>n</i>	GnT-V ^a	<i>P</i>	GnT-IX ^a	<i>P</i>
Tumor stage					
1, 2, 4s	57	2.23 \pm 0.29	0.021	1.78 \pm 0.25	0.21
3, 4	69	1.48 \pm 0.16		2.23 \pm 0.25	
<i>TrkA</i> expression					
High	59	2.11 \pm 0.27	0.010	1.86 \pm 0.17	0.75
Low	48	1.33 \pm 0.13		1.98 \pm 0.34	

^aMeans \pm S.E.M.

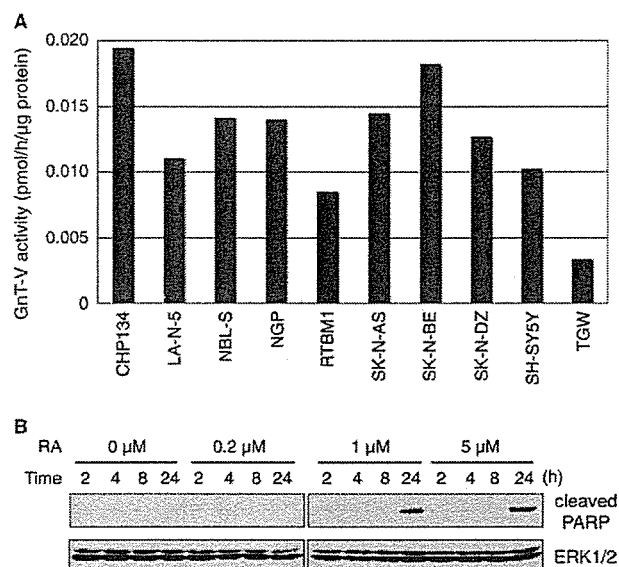


Fig. 2. GnT-V activities in various NBL cell lines and retinoic acid-induced apoptosis of CHP134 cells. (A) GnT-V activity of each of the NBL cells was measured using a whole cell lysate as an enzyme source. (B) Western blot of whole cell lysate of CHP134 cells. Cell apoptosis was observed by staining of cleaved PARP after treatment of retinoic acid (RA) at indicated concentrations and times. The expression levels of ERK1/2 were confirmed as a loading control.

in vivo [16,17]. Thus, we chose this cell line for further analysis of the effects of GnT-V on apoptosis.

3.3. Knockdown of GnT-V expression in CHP134 cells

We prepared a retroviral siRNA vector containing a small hairpin construct capable of generating a duplex RNAi oligonucleotide corresponding to human GnT-V. After retroviral infection, CHP134 cells were selected based on their resistance to G418, and clones with decreased GnT-V activities were chosen. The GnT-V activities were effectively downregulated by 80%, compared with those in parent or mock cells (Fig. 3A), while GnT-III activity, as a control, showed no significant changes between those cells. A quantitative real-time PCR analysis also indicated the downregulation of RNAi-directed

GnT-V mRNA expression in these cells (Fig. 3B). It is noteworthy that the cells in GnT-V-knockdown clones showed more spreading on the culture dishes, rather than the spindle shapes of the parent and mock cells (Fig. 4), suggesting that GnT-V may affect cellular cytoskeletal formation. In fact, Guo et al. reported that the overexpression of GnT-V in human HT1080 cells resulted in a decrease in cell adhesion on fibronectin [18].

3.4. Decreased susceptibility to retinoic acid-induced apoptosis in GnT-V-knockdown cells

To evaluate the effects of GnT-V expression on susceptibility to apoptosis induction in CHP134 cells, we examined cell viabilities in the presence of retinoic acid. After treatment with different concentrations of retinoic acid, we found that GnT-V-knockdown cells (KD1 and KD2 in Fig. 5A) had a tendency to be resistant to stimulation by retinoic acid. We further assessed the apoptosis level in retinoic acid-treated cells by PARP cleavage. The GnT-V-knockdown cells showed dramatically reduced levels of PARP cleavage (Fig. 5B). Collectively, these results suggest that GnT-V may sensitize cells to apoptotic signals, which partly contribute to the favorable prognosis of NBL.

4. Discussion

Previous studies demonstrated that an increased amount of β 1,6-branched oligosaccharides, formed by the action of GnT-V, are correlated with metastatic potential [2], and this has been shown to be a marker of tumor progression in human breast and colon neoplasia [19], and a prognostic marker in human colorectal carcinoma [20,21]. However, it is not always the case, as evidenced by the fact that Dosaka-Akita et al. reported that the lower expression of GnT-V is associated with a shorter survival and a poor prognosis in non-small cell lung cancers [22]. The present study also suggested that a higher expression of GnT-V is related to a favorable prognosis in NBLs.

GnT-V and GnT-IX, two closely related glycosyltransferases, are expressed in both the adult and fetal brain [7,9]. GnT-V expression is upregulated in E9.5 embryos, and is then

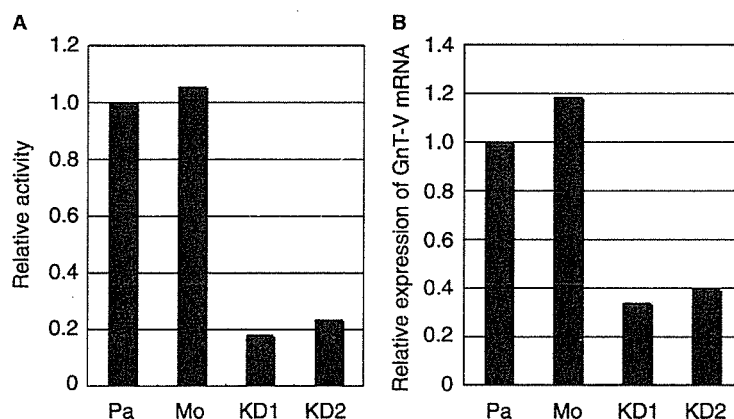


Fig. 3. Enzyme activities and mRNA expression levels in siRNA-mediated GnT-V-knockdown cells. (A) GnT-V activities of GnT-V-knockdown CHP134 cells. The microsomal fraction was used as an enzyme source in the assay. (B) mRNA expression of GnT-V in knockdown cells. Quantitative analysis was performed by real-time PCR. Pa, parent cells; Mo, mock cells; KD1 and KD2, GnT-V-knockdown cells.

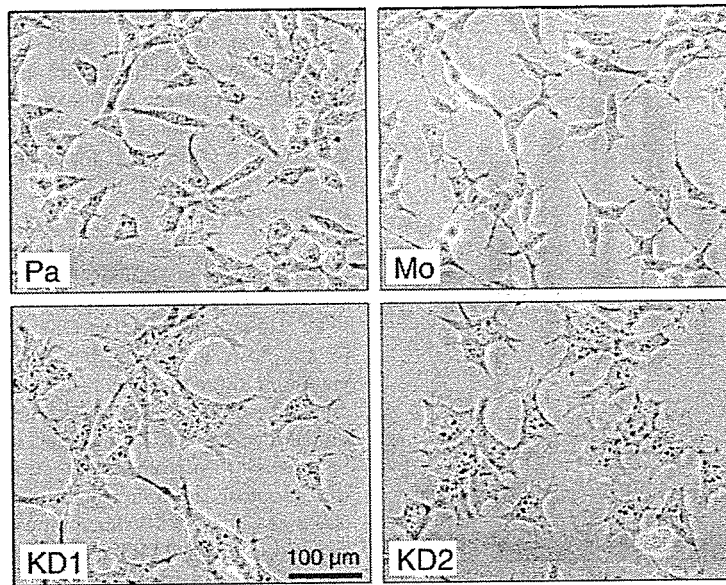


Fig. 4. Morphological changes in GnT-V-knockdown cells. Parent (Pa), mock (Mo), and GnT-V-knockdown CHP134 cells (KD1, KD2) were plated on culture dishes and incubated for 24 h in culture media. Cell shapes were observed by phase contrast microscopy.

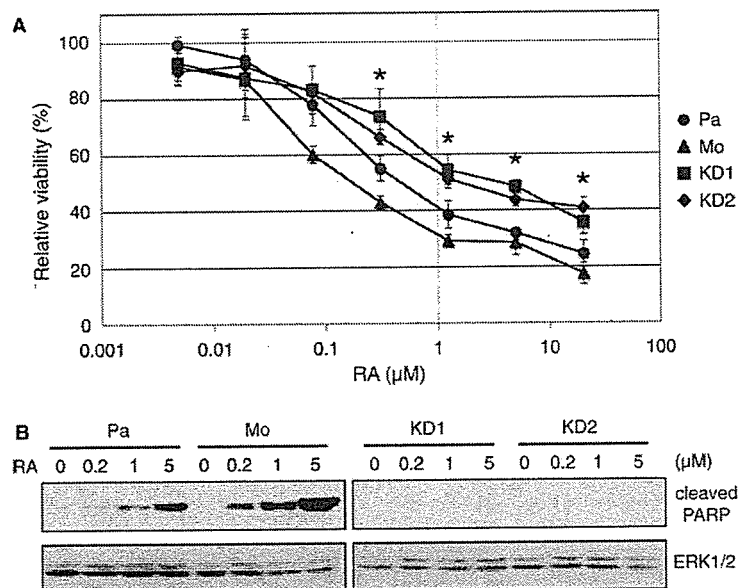


Fig. 5. Cell viabilities and PARP cleavage in retinoic acid-treated GnT-V-knockdown cells. Cell viabilities of parent (Pa), mock (Mo), and GnT-V-knockdown cells (KD1, KD2) were performed as described in Section 2 (A). Cells were treated with retinoic acid at the indicated concentrations for 3 days. * $P < 0.05$. (B) Western blot of cleaved PARP in a cell lysate using an anti-cleaved PARP antibody. Cells were harvested for analysis 24 h after retinoic acid-treatment.

restricted to regions comprised of several specialized epithelial cell layers and the neuroepithelium of the developing central nervous system [9]. On the other hand, GnT-IX is dominantly expressed in the human and mouse brain [7,23]. Thus, we attempted to examine the expressions of GnT-V and GnT-IX in primary NBL tissues.

The frequent gain of the chromosome 17q has been reported to be associated with a poor prognosis [24], and the preferential gain of the region from 17q22-qter indicated a dosage effect that provides a selective advantage to be aggressive NBLs [25].

The gene responsible for the selective advantage is unknown, but a candidate gene that is a member of the inhibitor of apoptosis proteins, survivin, which is mapped to 17q25, has been reported [14]. Although the GnT-IX gene is also mapped to 17q25 [7], an unequivocal correlation with prognosis was not observed in this study. Interestingly, a significant association between expression levels of GnT-V mRNA and the prognosis of 126 NBL patients was observed by real-time PCR analysis. Several human NBL cell lines also consistently express GnT-V. To understand the molecular mechanism associated with the

higher expression levels of GnT-V in the favorable prognosis of NBLs, we selected CHP134 cells as a cell model. Since the cell line is highly sensitive to retinoic acid-induced apoptosis [14,15], we compared the effects of retinoic acid on apoptosis between parent cells and GnT-V-knockdown cells.

In fact, GnT-V-knockdown cells showed a tendency to escape from retinoic acid-induced apoptosis, as confirmed by a cell viability assay and the extent of cleaved PARP, supporting the notion that a higher expression of GnT-V is correlated with a favorable prognosis of NBLs. It is noteworthy that a prominent morphological alteration with increased spreading was observed in the GnT-V-knockdown cells. The altered characteristic of GnT-V-knockdown CHP134 cells observed in this study is consistent with those of previous studies [3,18,26,27]. The overexpression of GnT-V enhances the metastatic potential in several cell types with reduced cell-matrix adhesion and increased motility [3,18,26]. Furthermore, GnT-V expression in human glioma cell line U-373 MG sensitizes these cells to drag-induced apoptosis [28]. Conversely, GnT-V null mouse embryonic fibroblasts exhibited an enhanced adhesion and spreading with associated reduced cell migration [27]. In addition, no significant effect of GnT-V overexpression was observed on apoptotic behavior in fibrosarcoma HT1080 cells, a fibroblast cell line, but a similar phenotypic change with regard to adhesion and migration has been reported [18]. In general, the adhesion of epithelial cells to extracellular matrices is weaker than that of fibroblast cells, and such adhesion is thought to be synergized with the signals of growth factor receptors for modulating cell proliferation and apoptosis. Therefore, we speculate that the GnT-V-induced decrease in cell adhesion could be a plausible factor responsible for the favorable prognosis in NBLs.

In conclusion, a correlation between higher expression levels of GnT-V with a favorable prognosis of NBL patients was found, and GnT-V may cause these tumors to regress by increasing their susceptibility to apoptosis.

Acknowledgments: This work was supported a Grant-in-Aid for Scientific Research (S) No. 13854010 from the Japan Society for the promotion of Science and by the 21st Century COE Program by the Ministry of Education, Science, Culture, Sports and Technology in Japan.

References

- [1] Hakomori, S. (2002) Glycosylation defining cancer malignancy: new wine in an old bottle. *Proc. Natl. Acad. Sci. USA* 99, 10231–10233.
- [2] Dennis, J.W., Laferte, S., Waghorne, C., Breitman, M.L. and Kerbel, R.S. (1987) Beta 1–6 branching of Asn-linked oligosaccharides is directly associated with metastasis. *Science* 236, 582–585.
- [3] Demetriou, M., Nabi, I.R., Coppolino, M., Dedhar, S. and Dennis, J.W. (1995) Reduced contact-inhibition and substratum adhesion in epithelial cells expressing GlcNAc-transferase V. *J. Cell. Biol.* 130, 383–392.
- [4] Granovsky, M., Fata, J., Pawling, J., Muller, W.J., Khokha, R. and Dennis, J.W. (2000) Suppression of tumor growth and metastasis in Mgat5-deficient mice. *Nat. Med.* 6, 306–312.
- [5] Saito, T., Miyoshi, E., Sasai, K., Nakano, N., Eguchi, H., Honke, K. and Taniguchi, N. (2002) A secreted type of beta 1,6-*N*-acetylglucosaminyltransferase V (GnT-V) induces tumor angiogenesis without mediation of glycosylation: a novel function of GnT-V distinct from the original glycosyltransferase activity. *J. Biol. Chem.* 277, 17002–17008.
- [6] Ihara, S., Miyoshi, E., Ko, J.H., Murata, K., Nakahara, S., Honke, K., Dickson, R.B., Lin, C.Y. and Taniguchi, N. (2002) Prometastatic effect of *N*-acetylglucosaminyltransferase V is due to modification and stabilization of active matrix by adding beta 1–6 GlcNAc branching. *J. Biol. Chem.* 277, 16960–16967.
- [7] Inamori, K., Endo, T., Ide, Y., Fujii, S., Gu, J., Honke, K. and Taniguchi, N. (2003) Molecular cloning and characterization of human GnT-IX, a novel {beta}1,6-*N*-acetylglucosaminyltransferase that is specifically expressed in the brain. *J. Biol. Chem.* 278, 43102–43109.
- [8] Kaneko, M., Alvarez-Manilla, G., Kamar, M., Lee, I., Lee, J.K., Troupe, K., Zhang, W., Osawa, M. and Pierce, M. (2003) A novel beta(1,6)-*N*-acetylglucosaminyltransferase V (GnT-VB). *FEBS Lett.* 554, 515–519.
- [9] Granovsky, M., Fode, C., Warren, C.E., Campbell, R.M., Marth, J.D., Pierce, M., Fregien, N. and Dennis, J.W. (1995) GlcNAc-transferase V and core 2 GlcNAc-transferase expression in the developing mouse embryo. *Glycobiology* 5, 797–806.
- [10] Brodeur, G.M. (2003) Neuroblastoma: biological insights into a clinical enigma. *Nat. Rev. Cancer* 3, 203–216.
- [11] Brodeur, G.M., Pritchard, J., Berthold, F., Carlsen, N.L., Castel, V., Castelberry, R.P., De Bernardi, B., Evans, A.E., Favrot, M. and Hedborg, F., et al. (1993) Revisions of the international criteria for neuroblastoma diagnosis, staging, and response to treatment. *J. Clin. Oncol.* 11, 1466–1477.
- [12] Kato, C., Miyazaki, K., Nakagawa, A., Ohira, M., Nakamura, Y., Ozaki, T., Imai, T. and Nakagawara, A. (2004) Low expression of human tubulin tyrosine ligase and suppressed tubulin tyrosination/detyrosination cycle are associated with impaired neuronal differentiation in neuroblastomas with poor prognosis. *Int. J. Cancer* 112, 365–375.
- [13] Taniguchi, N., Nishikawa, A., Fujii, S. and Gu, J.G. (1989) Glycosyltransferase assays using pyridylaminated acceptors: *N*-acetylglucosaminyltransferase III, IV, and V. *Meth. Enzymol.* 179, 397–408.
- [14] Islam, A., Kageyama, H., Takada, N., Kawamoto, T., Takayasu, H., Isogai, E., Ohira, M., Hashizume, K., Kobayashi, H., Kaneko, Y. and Nakagawara, A. (2000) High expression of Survivin, mapped to 17q25, is significantly associated with poor prognostic factors and promotes cell survival in human neuroblastoma. *Oncogene* 19, 617–623.
- [15] Takada, N., Isogai, E., Kawamoto, T., Nakanishi, H., Todo, S. and Nakagawara, A. (2001) Retinoic acid-induced apoptosis of the CHP134 neuroblastoma cell line is associated with nuclear accumulation of p53 and is rescued by the GDNF/Ret signal. *Med. Pediatr. Oncol.* 36, 122–126.
- [16] Nicholson, D.W., Ali, A., Thornberry, N.A., Vaillancourt, J.P., Ding, C.K., Gallant, M., Gareau, Y., Griffin, P.R., Labelle, M. and Lazebnik, Y.A., et al. (1995) Identification and inhibition of the ICE/CED-3 protease necessary for mammalian apoptosis. *Nature* 376, 37–43.
- [17] Tewari, M., Quan, L.T., O'Rourke, K., Desnoyers, S., Zeng, Z., Beidler, D.R., Poirier, G.G., Salvesen, G.S. and Dixit, V.M. (1995) Yama/ CPP32 beta, a mammalian homolog of CED-3, is a CrmA-inhibitable protease that cleaves the death substrate poly(ADP-ribose) polymerase. *Cell* 81, 801–809.
- [18] Guo, H.B., Lee, I., Kamar, M., Akiyama, S.K. and Pierce, M. (2002) Aberrant *N*-glycosylation of beta1 integrin causes reduced alpha5beta1 integrin clustering and stimulates cell migration. *Cancer Res.* 62, 6837–6845.
- [19] Fernandes, B., Sagman, U., Auger, M., Demetrio, M. and Dennis, J.W. (1991) Beta 1–6 branched oligosaccharides as a marker of tumor progression in human breast and colon neoplasia. *Cancer Res.* 51, 718–723.
- [20] Seelentag, W.K., Li, W.P., Schmitz, S.F., Metzger, U., Aeberhard, P., Heitz, P.U. and Roth, J. (1998) Prognostic value of beta1,6-branched oligosaccharides in human colorectal carcinoma. *Cancer Res.* 58, 5559–5564.
- [21] Murata, K., Miyoshi, E., Kameyama, M., Ishikawa, O., Kabuto, T., Sasaki, Y., Hiratsuka, M., Ohigashi, H., Ishiguro, S., Ito, S., Honda, H., Takemura, F., Taniguchi, N. and Imaoka, S. (2000) Expression of *N*-acetylglucosaminyltransferase V in colorectal cancer correlates with metastasis and poor prognosis. *Clin. Cancer Res.* 6, 1772–1777.

- [22] Dosaka-Akita, H., Miyoshi, E., Suzuki, O., Itoh, T., Katoh, H. and Taniguchi, N. (2004) Expression of *N*-acetylglucosaminyltransferase V is associated with prognosis and histology in non-small cell lung cancers. *Clin. Cancer Res.* 10, 1773–1779.
- [23] Inamori, K., Mita, S., Gu, J., Mizuno-Horikawa, Y., Miyoshi, E., Dennis, J.W. and Taniguchi, N. (in press) Demonstration of the expression and the enzymatic activity of *N*-acetylglucosaminyltransferase IX in the mouse brain. *Biochim Biophys Acta*.
- [24] Bown, N., Cotterill, S., Lastowska, M., O'Neill, S., Pearson, A.D., Plantaz, D., Meddeb, M., Danglot, G., Brinkschmidt, C., Christiansen, H., Laureys, G., Speleman, F., Nicholson, J., Bernheim, A., Betts, D.R., Vandesompele, J. and Van Roy, N. (1999) Gain of chromosome arm 17q and adverse outcome in patients with neuroblastoma. *N. Engl. J. Med.* 340, 1954–1961.
- [25] Lastowska, M., Cotterill, S., Bown, N., Cullinane, C., Variend, S., Lunec, J., Strachan, T., Pearson, A.D. and Jackson, M.S. (2002) Breakpoint position on 17q identifies the most aggressive neuroblastoma tumors. *Genes Chromosomes Cancer* 34, 428–436.
- [26] Yamamoto, H., Swoger, J., Greene, S., Saito, T., Hurh, J., Sweeley, C., Leestma, J., Mkrdichian, E., Cerullo, L., Nishikawa, A., Ihara, Y., Taniguchi, N. and Moskal, J.R. (2000) Beta1,6-*N*-acetylglucosamine-bearing *N*-glycans in human gliomas: implications for a role in regulating invasivity. *Cancer Res.* 60, 134–142.
- [27] Guo, H.B., Lee, I., Bryan, B.T. and Pierce, M. (2005) Deletion of mouse embryo fibroblast *N*-acetylglucosaminyltransferase V stimulates alpha5beta1 integrin expression mediated by the protein kinase C signaling pathway. *J. Biol. Chem.* 280, 8332–8342.
- [28] Dawson, G., Moskal, J.R. and Dawson, S.A. (2004) Transfection of 2,6 and 2,3-sialyltransferase genes and GlcNAc-transferase genes into human glioma cell line U-373 MG affects glycoconjugate expression and enhances cell death. *J. Neurochem.* 89, 1436–1444.

ORIGINAL ARTICLE

Increased expression of proapoptotic *BMCC1*, a novel gene with the *BNIP2* and *Cdc42GAP* homology (BCH) domain, is associated with favorable prognosis in human neuroblastomas

T Machida^{1,2,5}, T Fujita^{1,2,5}, ML Ooo¹, M Ohira¹, E Isogai¹, M Mihara^{1,2}, J Hirato³, D Tomotsune¹, T Hirata⁴, M Fujimori², W Adachi² and A Nakagawara¹

¹Division of Biochemistry, Chiba Cancer Center Research Institute, Chiba, Japan; ²Department of Surgery, Shinshu University School of Medicine, Matsumoto, Nagano, Japan; ³Department of Pathology, Gunma University School of Medicine, Maebashi, Gunma, Japan and ⁴Hisamitsu Pharmaceutical Co. Inc., Tokyo, Japan

Differential screening of the genes obtained from cDNA libraries of primary neuroblastomas (NBLs) between the favorable and unfavorable subsets has identified a novel gene *BCH* motif-containing molecule at the carboxyl terminal region 1 (*BMCC1*). Its 350 kDa protein product possessed a Bcl2-/adenovirus E1B nineteen kDa-interacting protein 2 (BNIP2) and Cdc42GAP homology domain in the COOH-terminus in addition to P-loop and a coiled-coil region near the NH₂-terminus. High levels of *BMCC1* expression were detected in the human nervous system as well as spinal cord, brain and dorsal root ganglion in mouse embryo. The immunohistochemical study revealed that *BMCC1* was positively stained in the cytoplasm of favorable NBL cells but not in unfavorable ones with *MYCN* amplification. The quantitative real-time reverse transcription-PCR using 98 primary NBLs showed that high expression of *BMCC1* was a significant indicator of favorable NBL. In primary culture of newborn mice superior cervical ganglion (SCG) neurons, *mBMCC1* expression was downregulated after nerve growth factor (NGF)-induced differentiation, and upregulated during the NGF-depletion-induced apoptosis. Furthermore, the proapoptotic function of *BMCC1* was also suggested by increased expression in CHP134 NBL cells undergoing apoptosis after treatment with retinoic acid, and by an enhanced apoptosis after depletion of NGF in the SCG neurons obtained from newborn mice transgenic with *BMCC1* in primary culture. Thus, *BMCC1* is a new member of prognostic factors for NBL and may play an important role in regulating differentiation, survival and aggressiveness of the tumor cells.

Oncogene (2006) 25, 1931–1942. doi:10.1038/sj.onc.1209225; published online 14 November 2005

Keywords: *BMCC1*; neuroblastoma; apoptosis; *BNIP2*; *Cdc42GAP*; *BCH* domain

Correspondence: Dr A Nakagawara, Division of Biochemistry, Chiba Cancer Center Research Institute, 666-2 Nitona, Chuoh-ku, Chiba 260-8717, Japan.

E-mail: akiranak@chiba-cc.jp

⁵These authors contributed equally to this work.

Received 13 April 2005; revised 15 September 2005; accepted 29 September 2005; published online 14 November 2005

Introduction

Neuroblastoma (NBL) is one of the most common pediatric neoplasms and originates from the sympathoadrenal lineage of neural crest. However, its biological as well as clinical behavior is highly heterogeneous. The tumors occurred in the patients under 1 year of age have a tendency to spontaneously regress or differentiate (Evans *et al.*, 1976). On the other hand, the tumors found in the patients more than 1 year of age are usually aggressive and often kill the patients. The latter subsets of the tumor frequently have multiple genomic aberrations which include frequent loss of the distal part of the short arm of chromosome 1, amplification of the *MYCN* oncogene, and gain of chromosome 17q, all of which are associated with unfavorable prognosis (Brodeur *et al.*, 1984; Caron, 1995).

Although the molecular mechanism underlying regression of NBL is still unclear, accumulating evidence suggests that the signals from neurotrophic factors and their receptors play an important role in regulating growth, differentiation and programmed cell death. High expression of *TrkA*, a high affinity receptor for nerve growth factor (NGF), is associated with the favorable outcome, and there is an inverse correlation between *TrkA* expression and *MYCN* amplification. Cells expressing functional *TrkA* may be susceptible to either programmed cell death leading to tumor regression, especially in infants, or to differentiation to a benign ganglioneuroma. Thus, like normal sympathetic neurons, a limited amount of NGF may be supplied from the stromal cells such as Schwann cells and fibroblasts, that at least partly regulates differentiation and programmed cell death of the NBL cells. In contrast, *TrkB*, another family member, is preferentially expressed in aggressive NBL cells together with its preferred ligands BDNF and NT-4/5 which stimulate proliferation in an autocrine/paracrine manner, conferring potency to invade and/or metastasize on the tumor cells (Nakagawara *et al.*, 1993, 1994).

The proto-oncogene *bcl-2* encodes a 25-kDa mitochondrial membrane protein that inhibits programmed cell death (Hockenbery *et al.*, 1990; Garcia *et al.*, 1992;

Oltvai *et al.*, 1993). The recent reports have suggested that *bcl-2* protein is expressed at relatively high levels in both NBLs and neural crest cells. However, the role of *bcl-2* in the regulation of differentiation and survival of NBL cells is still elusive.

In order to clarify the molecular mechanism of cellular signaling related to regression of NBL, we have cloned a large number of genes from full-length-enriched oligo-capping cDNA libraries constructed from two different subsets of NBL with favorable and unfavorable biology (Ohira *et al.*, 2003a, b). Sequence analysis of the genes from those libraries has revealed that the expression profile is significantly different between the both subsets. Screening by using semiquantitative RT-PCR has shown that more than 500 genes are differentially expressed between them. In the present paper, we report cloning and functional characterization of a novel gene termed as *Bcl2*-adenovirus E1B nineteen kDa-interacting protein 2 (*BNIP2*) and *Cdc42GAP* homology *BCH* motif-containing molecule at the carboxyl terminal region 1 (*BMCC1*), which is preferably expressed in favorable NBL.

Results

Full-length cDNA cloning and structural analysis of the *BMCC1* gene

As reported previously, we constructed oligo-capping cDNA libraries from different subsets of primary NBLs (Ohira *et al.*, 2003b). After DNA sequencing both ends of about 10 000 clones randomly picked up, we obtained 5000 independent genes, among which about 2000 were found to be novel by homology search. They were then subjected to semi-quantitative RT-PCR to examine if they are differentially expressed between favorable (stage 1, less than 1-year-old, single copy of *MYCN* and high expression of *TrkA*) and unfavorable (stage 3 or 4, more than 1-year-old, amplified *MYCN* and low expression of *TrkA*) subsets of NBL. The differential screening in a panel of template cDNAs obtained from 16 favorable and 16 unfavorable primary NBLs demonstrated an interesting novel gene (*Nbla00219*) which had a *BNIP2* and *BCH* domain, a recently reported new motif which might interact with *Bcl-2* protein, at the COOH-terminus. It was preferentially expressed in favorable NBLs.

Sequencing of the *Nbla00219* clone showed that the insert size was 2277 bp with a putative open reading frame (ORF) of 1452 bp (484 amino acids) localized at the 5'-end region. The database search demonstrated that the *Nbla00219* sequence matched to the *KIAA0367* cDNA (accession no.: AB002365) with 95% identity as well as a part of the genomic sequence within the BAC clone RP11-146P9 (GenBank accession no.: AL161625) which was mapped to chromosome 9p13. However, there was no in-frame stop codon in the upstream region of the putative initiation site of *KIAA0367*, suggesting that the coding region of the gene extended over the 5'-end. In fact, Northern blot analysis of human fetal brain mRNA using *nbla00219* cDNA as a probe demonstrated that the transcript size was approximately

12 kb (Figure 1d). In order to determine a full-length cDNA of this gene, we performed gene prediction according to the sequence information from the BAC clone RP11-146P9 by using several algorithm. The exons expected in the upstream region of the gene were confirmed by RT-PCR using cDNA libraries constructed from human fetal brain and/or NBL tissues with favorable prognosis as template with subsequent DNA sequencing. It revealed that the gene contained a large exon of about 6.5 kb within the extended 5'-coding region. The predicted 5'-side ORF was also confirmed by matching to the several mouse ESTs. Then, we finally identified the full-length *Nbla00219* cDNA (Figure 1a) with a 5'-untranslated region of 323 bp (nt. no. 1-323), an ORF of 8355 bp (nt. no. 324-8497), and a 3'-untranslated region of 3196 bp (nt. no. 8498-11 690) (accession no.: AB050197). The Kozak consensus sequence for translation initiation site (Kozak, 1987) was found at the putative ATG start codon (at position 324), though no in-frame stop codon was found in the upstream region. The blast search against public databases showed no significant homology except *BNIP2* (accession no.: XM007602, 52% identity) and *Cdc42GAP* (accession no.: NM004308, 38% identity) at the COOH-terminal end of the full-length *Nbla00219* (Figure 1a and b). Since the region had been termed as the *BCH* domain which was highly conserved among the three genes (Figure 1c), we named the full-length *Nbla00219* gene as *BMCC1*.

The *BCH* domain acts as the GTPase activating protein (GAP) in *BNIP2*. There are two critical arginine residues, Arg-236 and Arg-238, which are important for conferring the GAP activity to the *Cdc42* homodimers (Zhang and Zheng, 1998; Zhang *et al.*, 1999; Low *et al.*, 2000). In *BMCC1*, both critical arginine residues were well conserved. Using several algorithms to predict the secondary structure of amino acids and the intracellular localization, we found the coiled-coil motif (amino acids 918-941) and P-loop (amino acids 2293-2300) within the *BMCC1* protein (Figure 1a). Three putative transmembrane domains (amino acids 2545-2563, 2573-2597 and 2632-2653) were also suggested.

Although *BMCC1* was expressed significantly at higher levels in favorable than unfavorable NBLs, the expression levels of *BNIP2* family were similar between the NBL subsets (Figure 2a).

Expression of *BMCC1* in human tissues and cell lines

To study the expression pattern of *BMCC1* mRNA in human tissues, we performed semiquantitative RT-PCR. *BMCC1* was expressed in many tissues examined except for bone marrow, thymus and spleen (Figure 2c). The high levels of expression were seen in the nervous system (brain, cerebellum and spinal cord) as well as adrenal gland which were the tissues NBL originated from. We further performed semiquantitative RT-PCR to examine the expression levels of *BMCC1* in cultured cell lines including NBL and other cancers. *BMCC1* was expressed in most of 17 NBL cell lines tested (Figure 2b). Among the other cancer lines, high expression of *BMCC1* was observed in rhabdomyosar-

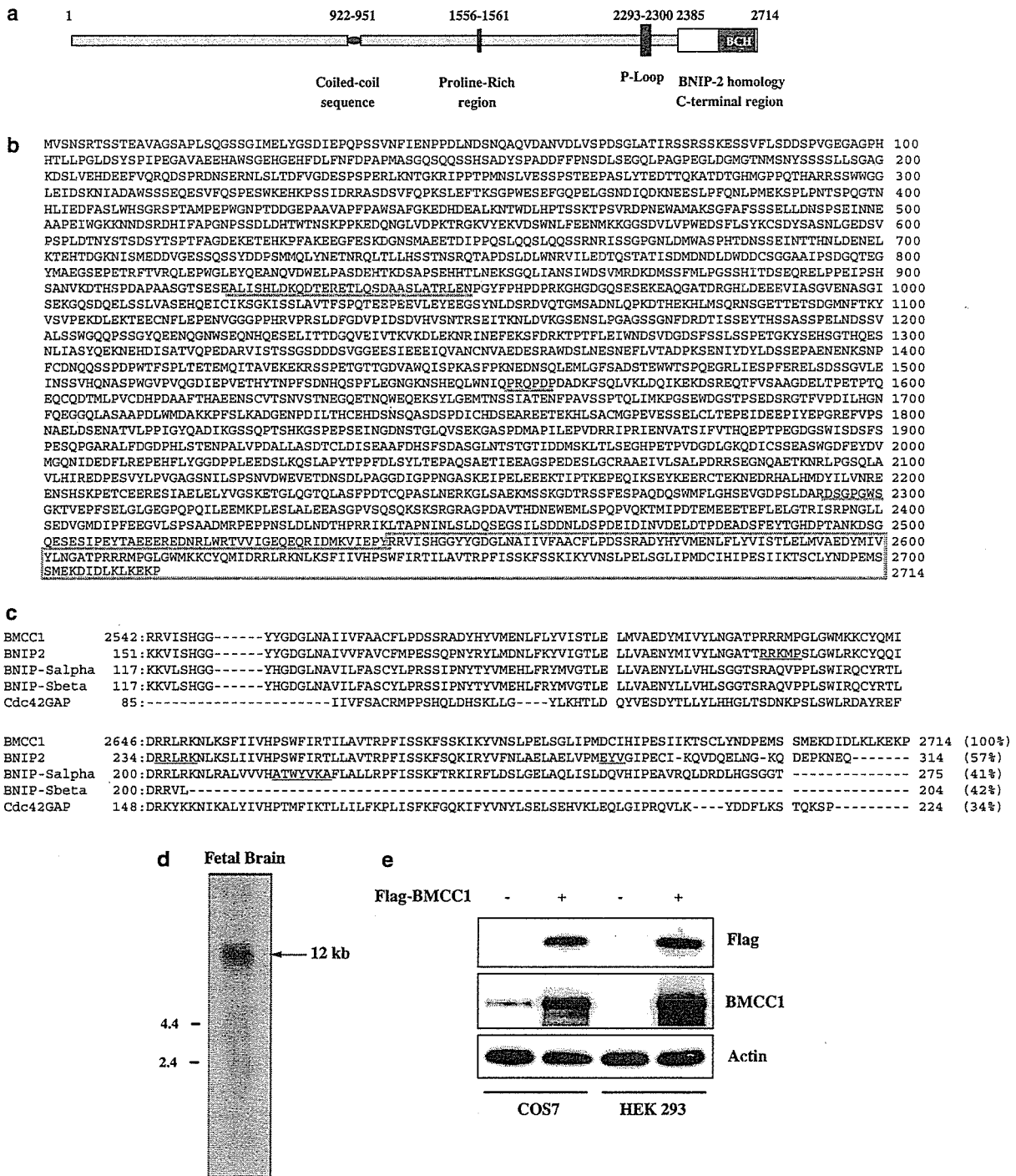


Figure 1 Molecular cloning of *BMCC1*. (a) Schematic structure of *BMCC1*. *BMCC1* contains coiled-coil sequence, proline-rich region, P-loop and BCH domain in its concurrent position. (b) Full-length amino-acid sequence of human *BMCC1*. Coiled-coil, proline-rich and P-loop regions were underlined and BCH domain was indicated in box. (c) Alignment of C-terminal regions of *BMCC1*, *BNIP-2*, *BNIP-Salpha*, *BNIP-Sbeta*, and *Cdc42GAP* homologous to BCH domain. Total number of amino-acid residues of each protein and their percent homology were described at the end of each sequence. RRRKMP (homophilic/heterophilic dimerized sequence), EYV (binding to switch I and insert region of *Cdc42*) (Low *et al.*, 2000) and RRLRK (arginine patch of BCH domain), ATWYVKA (binding motif for homophilic complex and critical for proapoptotic activity) (Zhou *et al.*, 2002), were underlined. (d) Northern blot analysis of *BMCC1* transcript in fetal brain tissue. Total RNA (25 μ g) purchased from Clontech was loaded for Northern blotting. Left; size markers showing 2.4 and 4.4 kb. (e) *BMCC1* expression in COS7 and HEK293 cells. pCAGGS-*BMCC1*-Flag was transfected into COS7 and HEK 293 cells and lysed after 48 h. Cell lysates were run into 8% SDS-PAGE in 35 mA for more than 4 h, transferred to immobilon-P membrane (MILLIPORE) and probed by anti-Flag, anti-*BMCC1* (C-terminal end epitope), and antiactin antibodies.

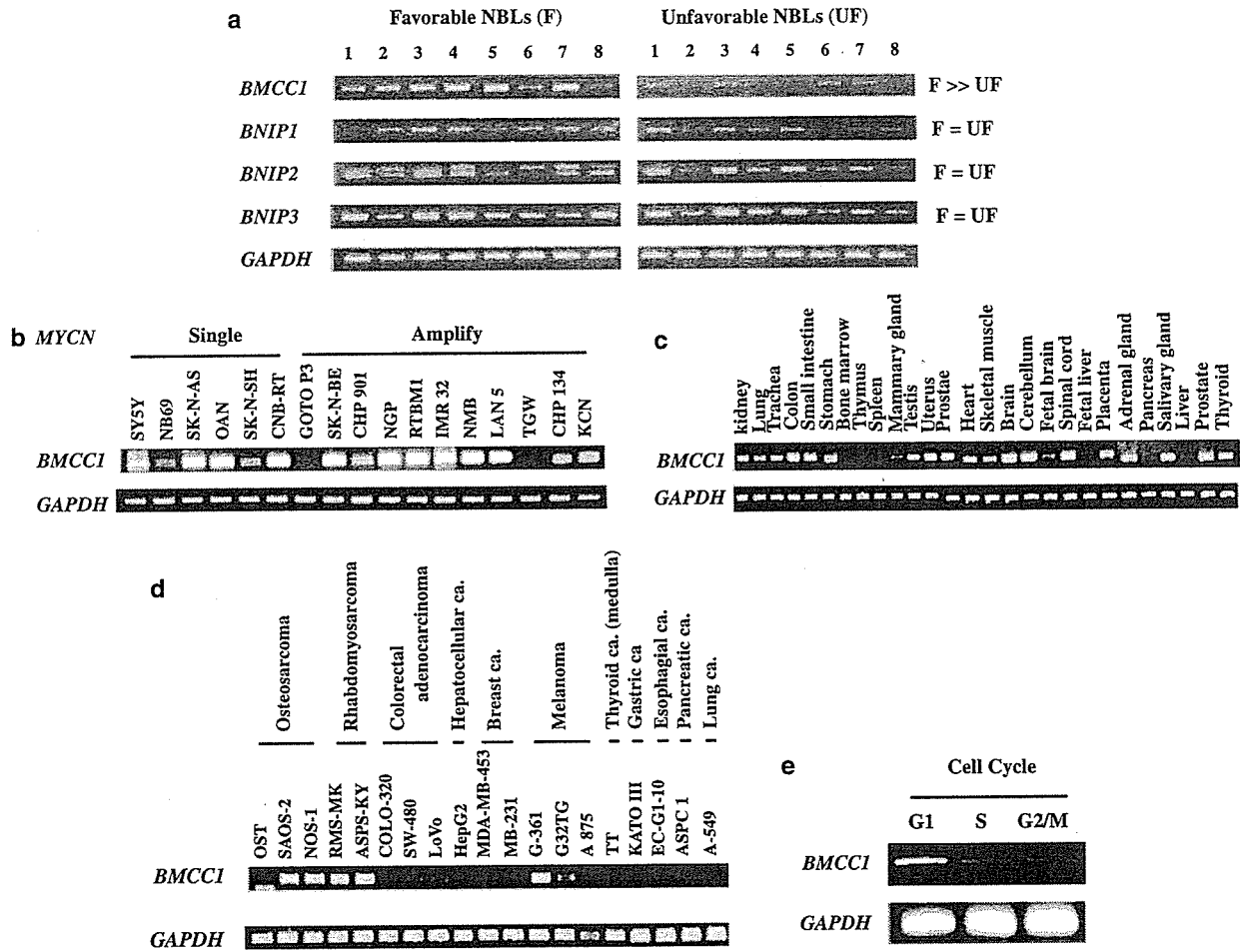


Figure 2 Expression of *BMCC1* mRNA. (a) Differential expression of *BMCC1* in favorable and unfavorable neuroblastomas. mRNA expression patterns for *BMCC1* and *BNIP* gene family members were detected by semiquantitative RT-PCR procedure. Results for eight favorable and eight unfavorable NBLs are shown. The expression of *GAPDH* is also shown as a control. Lanes 1-8: favorable NBLs (F; stage 1 or 2, with a single copy of *MYCN*), lanes 9-16: unfavorable NBLs (UF; stage 3 or 4, with *MYCN* amplification). (b) Expression of *BMCC1* mRNA in neuroblastoma cell lines. In all, 11 NBL cell lines with *MYCN* amplification and six cell lines with a single copy of *MYCN* were used for semiquantitative RT-PCR as templates. (c) Semiquantitative RT-PCR of *BMCC1* in multiple human tissues. Total RNA of 25 adult tissues and two fetal tissues were purchased from Clontech Co. Ltd. As a control, same cDNA templates were amplified by *GAPDH* primers. (d) Expression of *BMCC1* mRNA in the other cancer cell lines. Semiquantitative RT-PCR analysis was performed using cDNA primers and control *GAPDH* primers. Tumor origins were shown on the top. (e) The changes in expression of *BMCC1* at the cell cycle stages. HeLa cells were synchronized by treatment with 400 μ M mimosine for 18 h (G1-phase arrest), with 2 mM thymidine for 20 h (S-phase arrest), or with 0.6 μ g/ml nocodazole for 18 h (G2/M-phase arrest) and collected for RNA isolation. Semiquantitative RT-PCR was conducted by using *BMCC1* primers and *GAPDH* control primers.

coma, melanoma and some osteosarcoma cell lines, whereas only low levels of expression were found in cancer cell lines of liver, breast, thyroid and colon (Figure 2d). We further examined the cell cycle-dependent expression of *BMCC1* mRNA in HeLa cells by using semiquantitative RT-PCR. As shown in Figure 2e, *BMCC1* was predominantly expressed in G1 phase of the cell cycle.

In situ hybridization of BMCC1 in mouse embryo

In situ hybridization in mouse embryo showed that *BMCC1* was specifically expressed in neural tube and neural crest-related tissues. In E10.5 mouse embryo, *BMCC1* was highly expressed in neural tube and

pharyngeal arches which are derived from neural crest. The expression of *BMCC1* seemed to be more restricted in the later stages of development (Figure 3). In E12.5 mouse embryo (Figure 3d), *BMCC1* was expressed in spinal cord, hindbrain, midbrain, forebrain and dorsal root ganglia (DRG). Although the expressions of *BMCC1* in E14.5 mouse embryos (Figure 3a and b) were similar to those in E12.5, the regions expressing *BMCC1* in hindbrain (Figure 3a), spinal cord and forebrain at E14.5 (Figure 3b) were more dorsally restricted than at E12.5.

Immunohistochemical staining of BMCC1 in primary NBLs

The favorable NBLs occasionally expressed *BMCC1* in the cytoplasm of the tumor cells (Figure 4b). In contrast,

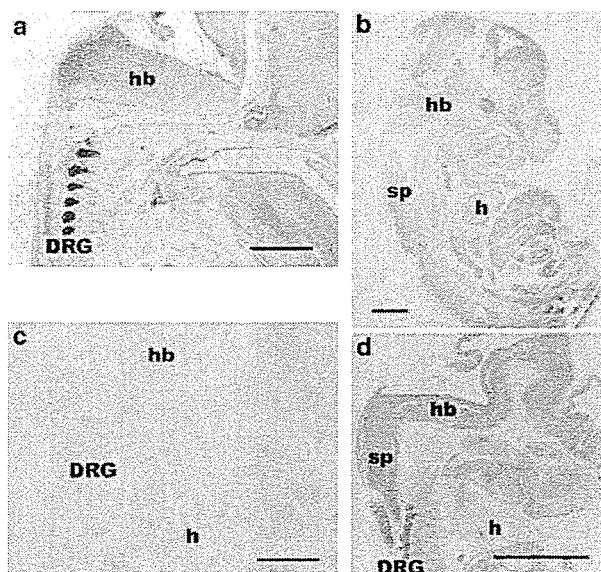


Figure 3 Section *in situ* hybridization of embryos with the *BMCC1* probe. Sagittal sections of embryos at E14.5 (a–c) and E12.5 (d) were prepared and the *BMCC1* expression was examined by section *in situ* hybridization. (a), (b) and (d) Antisense probes. (c) Sense probe (control). The *BMCC1* probe used is described in the Experimental procedures. DRG, dorsal root ganglion; sp, spinal cord; hb, hindbrain; h, heart. Scale bar, 200 μ m.

in the unfavorable neuroblastomas the tumor cells were entirely negative for *BMCC1* or only a few positive cells were observed (Figure 4d).

Prognostic significance of *BMCC1* mRNA expression in human NBLs

The levels of *BMCC1* mRNA expression were measured in 98 primary NBLs by using quantitative real-time RT-PCR. The high levels of *BMCC1* expression were significantly associated with favorable NBL in stages 1, 2 and 4 (Figure 4e). The high levels of *BMCC1* expression was significantly associated with young age ($P < 0.00005$), favorable stages ($P < 0.00005$), high expression of *TrkA* mRNA ($P < 0.00005$), single copy of *MYCN* ($P < 0.00005$), tumors found by mass screening (MS) ($P < 0.00005$), nonadrenal origin ($P = 0.0025$) according to the Student's *t*-test. The log-rank test showed that the high expression of *BMCC1* was significantly correlated with a favorable outcome ($P = 0.0008$) as shown in the Kaplan–Meier cumulative survival curves (Table 1 and Figure 4f).

The multivariate Cox regression analysis also demonstrated that *BMCC1* expression (high vs low), age (<1 year vs ≥ 1 year), *MYCN* copy number (1 copy vs >1 copy), and MS (positive tumors vs sporadic tumors) had prognostic significance ($P < 0.0005$) (Table 2). *BMCC1* expression was significantly related to survival ($P = 0.007$) after controlling age ($P = 0.018$). However, it lost significance in a model including jointly with *MYCN* amplification or MS. Furthermore, *BMCC1* expression was significantly related to survival

($P = 0.027$) after controlling age ($P = 0.014$) and origin ($P = 0.403$).

Changes in *BMCC1* mRNA expression during neuronal differentiation and apoptosis

To examine whether exogenous expression of *BMCC1* affects the cell growth of neuronal PC12 cells, a rat pheochromocytoma cell line, we transfected the cells with a full-length *BMCC1* cDNA. The overexpression of *BMCC1* appeared to decrease the cell growth but the result was not statistically significant (data not shown). We then tested if expression of *BMCC1* mRNA was changed during neuronal differentiation and/or apoptosis. For that purpose, we used three different neuronal cell lines. The NT2 cell line, which was established from human immature teratocarcinoma and the cells show astrocytic differentiation after treatment with retinoic acid (RA) (Moasser *et al.*, 1996). The CHP134 NBL cells undergo apoptosis after 3 days of the treatment with RA (Islam *et al.*, 2000). On the other hand, the RTBM1 human NBL cells are induced to differentiate after the treatment with RA (Nakamura *et al.*, 1998). We have confirmed that caspase 3 expression was increased in CHP134 cells but decreased in RTBM1 cells at day 7 after treatment with RA by semiquantitative RT-PCR. On the other hand, nestin expression was not changed in the former and slightly increased in the latter (Figure 5a). Expression of *BMCC1* mRNA was downregulated during RA-induced neuronal differentiation in both NT2 and RTBM1 cells, whereas it was rather upregulated in CHP134 cells on day 7 after the treatment with RA when many cells were undergoing apoptosis (Figure 5a).

To further confirm the above observation seen in neuronal cell lines, we examined the changes in *BMCC1* expression in superior cervical ganglion (SCG) neurons obtained from newborn mice in primary culture. The cultured cells were treated with 50 ng/ml NGF for 5 days (induction of neuronal differentiation) and then depleted NGF from the medium and added anti-NGF antibodies to induce neuronal apoptosis. As shown in Figure 5b, induction of differentiation by NGF decreased expression of *BMCC1*, whereas the NGF-depletion-induced apoptosis was accompanied with increase in *BMCC1* expression. This was very similar to the changes in expression of *c-jun* and *Bim* which had already been reported (Whitfield *et al.*, 2001). Thus, the levels of *BMCC1* mRNA are changed during neuronal differentiation and apoptosis in an opposite manner.

Enhanced NGF-depletion-induced apoptosis in SCG neurons obtained from *BMCC1* transgenic mice

We next generated *BMCC1* transgenic mice by using the expression construct with the tyrosine hydroxylase promoter-driven promoter to examine the functional role of *BMCC1* in the sympathetic neurons. The SCG neurons obtained from either control or transgenic newborn mice were subjected to primary culture. The integration of the *BMCC1* in the mouse genome and its overexpression in SCG neurons were confirmed by both

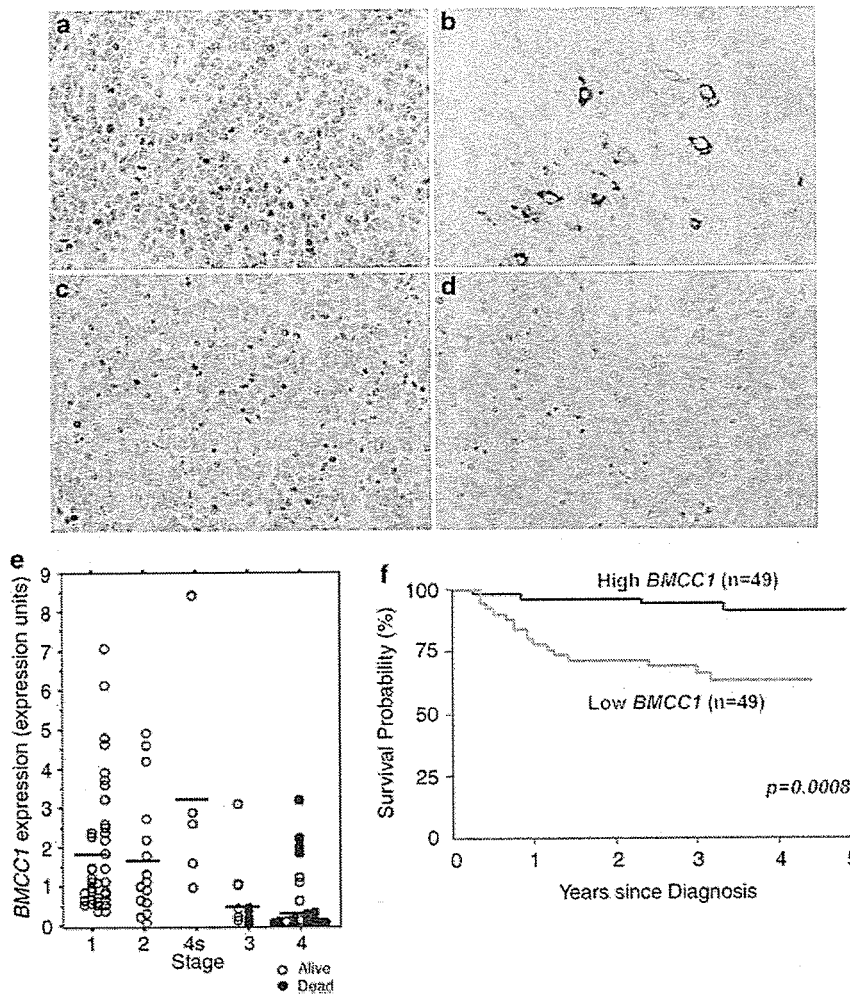


Figure 4 Immunohistochemistry and prognostic significance of *BMCC1* expression in primary neuroblastomas. (a) and (b) In the favorable neuroblastoma without *MYCN* amplification, the tumor cells are occasionally positive for *BMCC1* in the cytoplasm. (c) and (d) The unfavorable neuroblastoma with *MYCN* amplification is negative for *BMCC1*. (a) and (c) Hematoxylin–eosin staining. (b) and (d) *BMCC1* immunostaining. (e) Low expression of *BMCC1* is associated with poor prognosis of the patients with neuroblastoma. Real-time quantitative RT–PCR analysis of *BMCC1* in 98 tumor samples from patients with neuroblastomas according to tumor stage. The levels of expression of *BMCC1* were normalized to that of *GAPDH*. Horizontal lines; group means, open circles; patients alive, solid circles, patients deceased. (f) Cumulative survival curves of patients with neuroblastoma, according to expression of *BMCC1* mRNA. The Kaplan–Meier curves show the probability of survival in terms of the level of expression of *BMCC1*. The survival curves were analysed by the Mantel–Haenszel log-rank test.

RT–PCR (Figure 6a) and Western blot (data not shown). The treatment of the transgenic SCG neurons with NGF in primary culture induced neurite extension similarly to control cells, but induction of apoptosis after depleting NGF was significantly enhanced in the cells overexpressing *BMCC1* (Figure 6b–d). This suggested that *BMCC1* overexpression may function as proapoptotic in neuronal cells.

Discussion

The presence of the highly conserved BCH domain in *BMCC1* suggests its role in the regulation of apoptosis. *BNIP2*, which shares the BCH domain with *BMCC1*, has originally been identified as a molecule interacting

with the adenovirus E1B 19-kDa protein. The E1B protein protects the cells from apoptosis induced by viral infection or other proapoptotic stimuli (Gooding *et al.*, 1991; Hashimoto *et al.*, 1991; White *et al.*, 1992; Boyd *et al.*, 1994). *Bcl-2* and its related antiapoptotic proteins can functionally substitute for the E1B 19-kDa protein and bind to *BNIP2*. Therefore, it has been suggested that *BNIP2* is a potential proapoptotic protein (Subramanian *et al.*, 1995).

On the other hand, *Cdc42* regulates the activation of the c-Jun amino-terminal kinase (*JNK*) in various cells (Bagrodia *et al.*, 1995; Coso *et al.*, 1995; Zhang *et al.*, 1995). *Cdc42* induces an apoptosis mediated by the *JNK*–*MAP* kinase cascade in Jurkat T lymphocytes (Chuang *et al.*, 1997). The apoptosis is prevented by inhibitors of caspases, suggesting that activation of the

Table 1 Prognostic significance of *BMCC1* expression, age, stage, *TrkA* expression, *MYCN* amplification, mass screening and tumor origin in primary neuroblastomas (log-rank tests)

Variable	t-tests			Log-rank tests		
	Number of patients	Mean ± s.e.m. (<i>BMCC1</i> exp.)	P-value	Number of deaths	Number of expected deaths	P-value
<i>BMCC1</i> expression						0.0008
Low	49			17	9.39	
High	49			4	11.61	
Age (year)						<0.00005
<1	63	1.82 ± 0.23	<0.00005	5	14.55	
≥1	35	0.64 ± 0.15		16	6.45	
Tumor stage						<0.00005
1, 2, 4s	59	1.97 ± 0.23	<0.00005	0	14.57	
3, 4	39	0.55 ± 0.13		21	6.43	
<i>TrkA</i> expression						<0.00005
Low	44	0.91 ± 0.22	<0.00005	21	7.75	
High	54	1.81 ± 0.25		0	13.25	
<i>MYCN</i> copy number ^a						<0.00005
Amplified	27	0.30 ± 0.10	<0.00005	18	4.14	
Single	70	1.80 ± 0.20		3	16.86	
Mass screening						<0.00005
Positive	55	1.87 ± 0.22	<0.0025	1	13.32	
Negative	43	0.80 ± 0.22		20	7.68	
Origin						0.061
Adrenal gland	62	1.11 ± 0.20	<0.00005	17	12.82	
Others	36	1.91 ± 0.25		4	8.18	

^aOne patient who had missing *MYCN* information was excluded from analysis.

JNK pathway by Cdc42 is regulated by caspases. The interactive regulation between activation of JNK pathway and that of caspase cascade has also been reported in other biological systems (Cahill *et al.*, 1996; Juo *et al.*, 1997; Lenczowski *et al.*, 1997; Seimiya *et al.*, 1997). Cdc42 is also known to function as an initiator of neuronal cell death by activating a c-Jun-regulated transcriptional machinery (Bazenet *et al.*, 1998). Cdc42GAP is a Cdc42-activating protein and, like Cdc42, binds to BNIP2 through the BCH domain when it is dephosphorylated at the tyrosine residue. Thus, the proteins with the BCH domain including *BMCC1* seem to function in the regulation of apoptosis. The 'EYV' motif in the BCH domain, which is necessary for binding BNIP2 and Cdc42, is also conserved in the same domain of *BMCC1*. The role of P-loop in the regulation of apoptosis may also be important. Recently, it has been reported that ARTS (apoptosis-related protein in the TGF- β signaling pathway) mediates apoptosis through its P-loop motif. ARTS is a member of the septin family, localizes in cellular mitochondria and plays a role in regulating apoptosis. The P-loop consensus sequence is found in the proapoptotic protein, Apaf-1/CED-4 (Yuan and Horvitz, 1992; Zou *et al.*, 1997; Larisch *et al.*, 2000). It is interesting that *BMCC1* also possesses a P-loop motif, also suggesting its proapoptotic function.

The biological importance of BNIP2 has been reported in the neuronal system. Expression of BNIP2

is developmentally regulated during the maturation of rat brain (Zou *et al.*, 1997). The recent reports suggest that expression of *BNIP2* is downregulated by the treatment of NBL cells with estrogen (Garnier *et al.*, 1997), and that both estrogen and progesterone promote survival of NBL cells through the BNIP2 function during the apoptosis induced by TNF- α (Vegeto *et al.*, 1999). Furthermore, BNIP2 has been identified to be a putative downstream substrate of the FGF receptor tyrosine kinase signaling and possesses GTPase-activating activity to Cdc42. Thus, BNIP2 as well as Cdc42GAP seems to play a role in controlling the intracellular signals of neuronal differentiation and apoptosis.

However, our present results show that, among the molecules with the BCH domain, only *BMCC1*, but not *BNIP2* or *Cdc42GAP*, is differentially expressed among the NBL subsets, significantly at higher levels in favorable tumors than the aggressive ones. This suggests that *BMCC1*, rather than *BNIP2* or *Cdc42GAP*, is functioning *in vivo* in favorable NBLs undergoing neuronal differentiation and/or programmed cell death. The importance of *BMCC1* in NBL cell death has also been demonstrated in the study using neuronal cell lines. The RA-induced apoptosis of CHP134 NBL cells is accompanied with increased expression of *BMCC1*, while induction of differentiation in RTBM1 cells rather decreases its mRNA level. In the former system, the RA-triggered apoptosis induced upregulation of both

Table 2 Cox regression models using *BMCC1* expression and dichotomous factors of age, *MYCN* amplification, mass screening and tumor origin (*n* = 98)

Model	Variable	P-value	HR (95% CI)	Variable	P-value	HR (95% CI)	Variable	P-value	HR (95% CI)
A	<i>BMCC1</i> exp. (log)	<0.0005	0.53 (0.40, 0.70)						
B	Age (≥ 1 vs <1 year)	<0.0005	7.5 (2.72, 20.7)						
C	<i>MYCN</i> (1 copy vs >1 copy)	<0.0005	0.035 (0.0099, 0.12)						
D	Mass screening (+ vs -)	<0.0005	0.028 (0.0037, 0.21)						
E	Origin (adrenal vs others)	0.072	2.7 (0.91, 8.08)						
F	<i>BMCC1</i> exp. (log)	0.007	0.55 (0.47, 0.89)	Age (≥ 1 vs <1 year)	0.018	3.9 (1.26, 12.0)			
G ^a	<i>BMCC1</i> exp. (log)	0.72	1.05 (0.77, 1.47)	<i>MYCN</i> (1 copy vs >1 copy)	<0.0005	0.03 (0.0071, 0.13)			
H	<i>BMCC1</i> exp. (log)	0.079	0.77 (0.57, 1.03)	Mass screening (+ vs -)	0.003	0.04 (0.0053, 0.34)			
I	<i>BMCC1</i> exp. (log)	<0.0005	0.55 (0.41, 0.74)	Origin (adrenal vs others)	0.59	1.38 (0.42, 4.46)			
J	<i>BMCC1</i> exp. (log)	0.027	0.59 (0.49, 0.96)	Age (≥ 1 vs <1 year)	0.014	4.1 (1.33, 12.9)	Origin (adrenal vs others)	0.403	1.5 (0.51, 5.32)

^aOne patient who had missing *MYCN* information excluded from the analysis. All variables were grouped into two categories, except *BMCC1* expression (log). HR, hazard ratio; 95% CI, confidence interval.

p21^{WAF1} and *caspase-3*, and downregulation of survivin. The downregulation and upregulation of *BMCC1* expression was also observed in the newborn mouse SCG cells undergoing NGF-induced differentiation and NGF-depletion-induced apoptosis in primary culture, respectively. Furthermore, in SCG neurons obtained from newborn transgenic mice for *BMCC1*, NGF-depletion-induced apoptosis was significantly enhanced. Thus, these results strongly suggest that *BMCC1* is stimulated or acts as a proapoptotic factor when the neuronal cell death is induced.

BMCC1 mRNA is induced at G1 phase of the cell cycle. The physiological significance of the cell cycle-dependent expression of *BMCC1* is currently unclear. However, activated Cdc42, a *BMCC1*-related molecule, also induces G1 cell cycle progression in quiescent Swiss 3T3 fibroblasts (Yamamoto *et al.*, 1993; Olson *et al.*, 1995) and upregulates E2F transcriptional activity in NIH3T3 cells to induce accumulation of cyclin D1 and hyperphosphorylation of RB protein (Gjoerup *et al.*, 1998). *BMCC1* may also play a role in G1-phase progression of the cell cycle via unknown mechanism.

Our statistical analysis has strongly suggested the importance of *BMCC1* expression in predicting the prognosis of NBLs. The *BMCC1* expression is upregu-

lated in favorable NBLs and downregulated in unfavorable, advanced stages of NBLs. The similar pattern of expression in NBLs has also been reported in *TrkA* (Nakagawara *et al.*, 1993, 1994; Nakagawara, 1998, 2001), *c-Ha-Ras* (Tanaka *et al.*, 1998), *CD44* (Favrot *et al.*, 1993) and *pleiotrophin* (Nakagawara *et al.*, 1995). Here, we have added expression of *BMCC1*, at either mRNA or protein level, as a new prognostic indicator of favorable NBLs. Furthermore, our preliminary result has suggested that activated *TrkA* physically interacts with *BMCC1*, which in turn regulates the downstream signaling to control growth, differentiation and survival of neuronal cells (unpublished data). Therefore, *BMCC1* could be a key regulator of *TrkA*-activation-mediated intracellular signaling pathway in favorable NBLs, that is defective in aggressive tumors such as those with *MYCN* amplification. Thus, *BMCC1* might be an important molecular tool to develop new therapeutic strategy against aggressive NBLs.

Materials and methods

Patients

We studied tumors from 98 children with NBL which had been diagnosed between 1995 and 1999. In all, 55 patients were

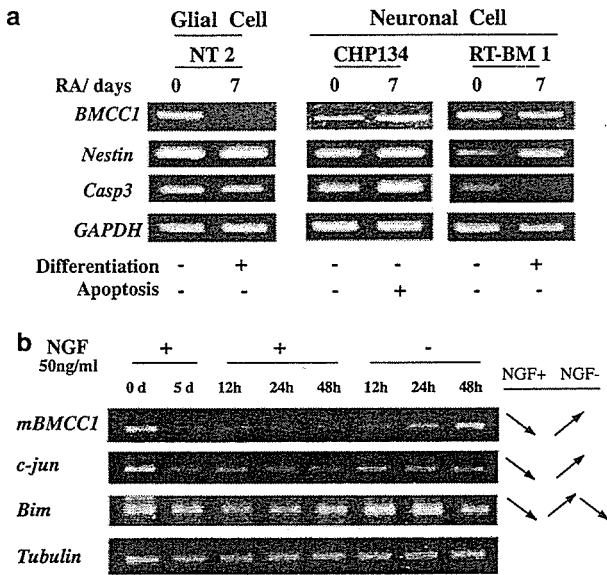


Figure 5 Expression of *BMCC1* during differentiation and apoptosis on neuronal cells. (a) The changes in *BMCC1* expression during induction of differentiation and apoptosis in neuronal cell lines. Two neuroblastoma cell lines (CHP134 and RTBM1) and teratocarcinoma cell line NT2 were treated with 5 μ M all-*trans* retinoic acid (RA) or were cultured in the serum-free RPMI1640 medium for 7 days. Semiquantitative RT-PCR was performed using *BMCC1* primers and control *GAPDH* primers. (b) The changes in mRNA expression of mouse *BMCC1* during NGF-induced differentiation and NGF-depletion-induced apoptosis. Mouse superior cervical ganglion (SCG) cells were cultured with NGF for 5 days and were further cultured with or without NGF for indicated intervals (12, 24 and 48 h) (see Figure 6b, upper panels). *Tubulin* primers were used for standardization of the cDNA concentration for semiquantitative RT-PCR. *c-jun* and *Bim* were also used for positive controls.

identified by a MS program started in 1985. The selection of tumors for this study was solely based on the availability of a sufficient amount of tumor tissue, from which DNA and RNA could be prepared for the analyses described below. The diagnosis of NBL was confirmed by histologic assessment of the tumor specimen obtained at surgery according to the Shimada's classification (Shimada *et al.*, 1984). The tumors were staged according to the International NBL Staging System (INSS) (Brodeur *et al.*, 1993). In all, 39 tumors were stage 1, 15 stage 2, five stage 4, 10 stage 3 and 29 stage 4. The patients were treated according to the protocols previously described (Kaneko *et al.*, 1998).

Tumor samples and cell lines

Fresh, frozen tumorous tissues were sent to the Division of Biochemistry, Chiba Cancer Center Research Institute, from various hospitals in Japan with informed consent from the patients' parents. All samples were obtained by surgery (or biopsy) and stored at -80°C . Studies were approved by the Institutional Review Board of the Chiba Cancer Center. Human cell lines which we used, except for COS-7, HEK 293 and HeLa cells, were cultured in the RPMI1640 medium (Nissui Pharmaceutical Co. Ltd, Tokyo, Japan) with 10% fetal bovine serum (FBS, Invitrogen Corp.) and 50 $\mu\text{g}/\text{ml}$ penicillin/streptomycin (Invitrogen Corp.) at humidified 5%

$\text{CO}_2/95\%$ air at 37°C . COS-7, HEK 293, and HeLa cells were grown in Dulbecco's modified Eagle's medium (DMEM) supplemented with 10% (v/v) FBS, 2 mM L-glutamine (Nissui Pharmaceutical Co. Ltd), 50 U/ml penicillin, and 50 $\mu\text{g}/\text{ml}$ streptomycin.

Treatment of cell lines with RA

NT2, CHP134 and RTBM1 were seeded at a density of 1×10^6 cells per 10 cm tissue culture dish in the presence of 5 μM RA on the day of induction. The cells were grown for 7 days with substituting for culture medium with RA every other day. Total cellular RNA for preparing the RT-PCR templates was extracted after culturing for 7 days.

Cell cycle analysis

Approximately 50–70% confluent of HeLa cells were treated each by 400 μM mimosine for 18 h (G1 arrest), 2 mM thymidine for 20 h (S arrest), and 0.6 $\mu\text{g}/\text{ml}$ nocodazole for 18 h (G2/M arrest). After confirmation of a synchronization of cultured cells by FACS, total RNA was extracted and the expression of *BMCC1* was examined by RT-PCR.

Northern blot analysis

Total RNA (25 μg) prepared from cell lines was electrophoresed in 1% agarose-formaldehyde gels and transferred to a nylon membrane. For the hybridization probe, 1.5 kb fragment in 3' part of *BMCC1* was used. Hybridization and washing were performed as described previously (Nagai *et al.*, 2000).

Transfection and antibodies

Cells at 90% confluence in 60-mm plates were transfected with indicated plasmids using FuGENE 6 transfection reagent (Roche) for COS-7 and Lipofectamine 2000 reagent (Invitrogen) for HEK 293 cells according to their manufacturer's instructions. To generate the BMCC-1-specific antibody, rabbit antiserum was raised against the peptides individually (residues 31–59, 836–858, 993–1022, 1378–1402, 1719–1737, 2180–2209, 2693–2714) of human BMCC1. The antibody specific to C-terminal end of BMCC1 is crossreacted to human (transfectants), mouse (Neuro 2A) and rat (PC12) BMCC-1. Antiactin IgG (polyclonal) was purchased from Sigma, St Louis, MO, USA.

Semiquantitative RT-PCR

For semiquantitative RT-PCR analysis, 5 μg of total RNAs were converted to cDNA using random primers by Superscript II reverse transcriptase (Gibco-BRL). In all, 2 μl of the 100-fold dilution of cDNA was subjected to PCR. The 20 μl of PCR reaction mixture contained 1 μM forward and reverse primer specific for *BMCC1*, 250 μM deoxynucleotide triphosphates (dNTPs), 50 mM KCl, 10 mM Tris-HCl (pH 8.0), 1.5 mM MgCl_2 and 0.5 U Taq DNA polymerase (TAKARA, Otsu, Japan). The PCR amplification was carried out for 35 cycles (preheat at 95°C for 2 min, denature at 95°C for 15 s, annealing at 58°C for 15 s, and extension at 72°C for 20 s) in thermocycler (Perkin-Elmer Cetus, Foster City, CA, USA). The PCR products were electrophoresed in 2.5% agarose gel, and visualized by UV illuminator. *BMCC1* primer sequences were as follows; forward: 5'-CGTTTATTTGCCGGTAGG AG-3', reverse: 5'-GCTCAGGCTCTTTGGTAGGA-3'. As a control, *GAPDH* primers (forward primer; 5'-CTGCACCAA CAATATCCC-3', reverse primer; 5'-GTAGAGACAGGG TTTTAC-3') were also used with reduced cycle (28 cycles).

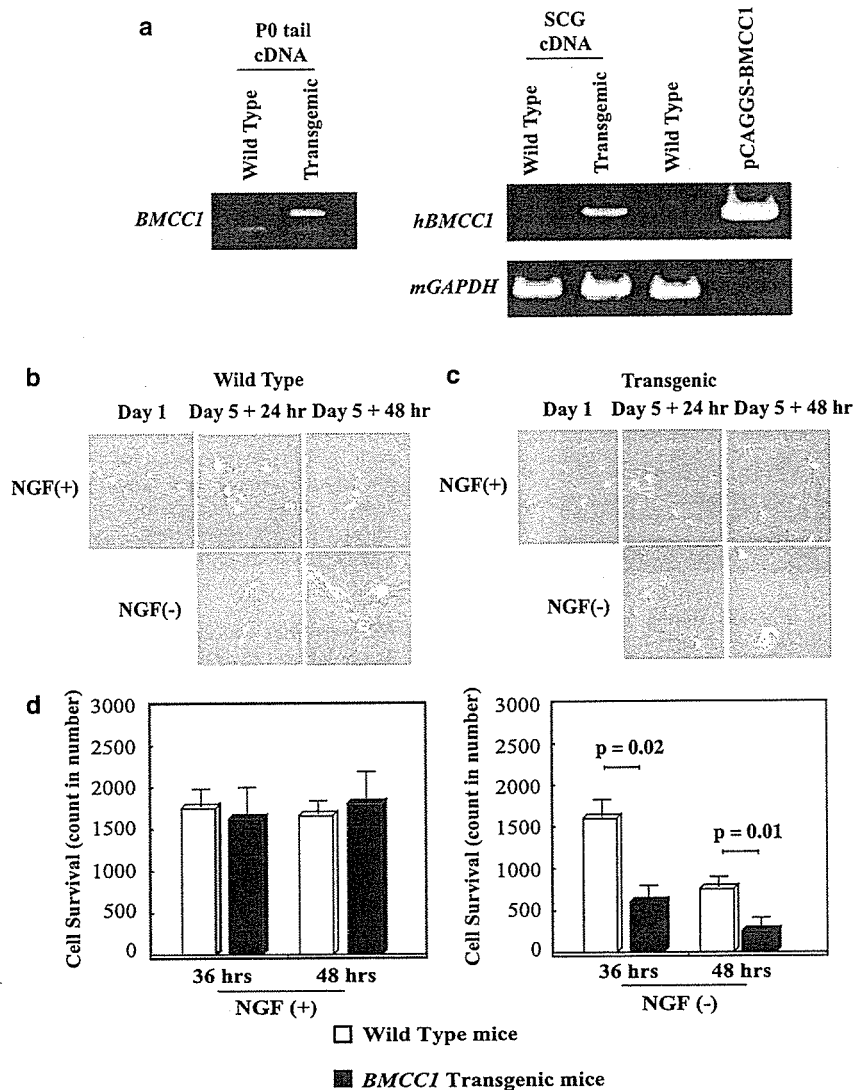


Figure 6 Increased apoptosis in superior cervical neurons obtained from newborn mice transgenic with the tyrosine hydroxylase promoter-driven human *BMCC1* in primary culture. (a) Expression of human *BMCC1* in SCG neurons obtained from *BMCC1* transgenic mice. SCG from both side of submandibular region was dissected from P₁ mice of wild-type and transgenic mice within 24 h after birth (described in Materials and methods). mRNA was purified from SCGs by using Trizol solution and RT-PCR was performed to confirm *BMCC1* expression. Genotyping by PCR is shown in left panel. (b) and (c) Morphological changes in SCG neurons after treating with NGF and withdrawal of NGF. The SCG cells were obtained from wild-type (b) and *BMCC1* transgenic (c) newborn mice. The cells were cultured in the presence of 50 ng/ml NGF for 5 days and were continuously treated with or without 50 ng/ml NGF for the following 2 days as described in Materials and methods. (d) Enhanced apoptosis in *BMCC1* transgenic SCG neurons after depletion of NGF. Numbers of survived SCG cells were counted at 36 and 48 h after NGF depletion. Values are shown as the means \pm s.e.m. from triplicate cultures. Similar results were obtained in two additional independent experiments.

Quantitative real-time PCR analysis

For quantification of *BMCC1* in primary NBL, cDNA was synthesized with random primers by Superscript II reverse transcriptase (Gibco-BRL) from 15 μ g of primary tumor total RNA. The following primers and probe were used; forward primer 5'-GGACAGTGGTCATTGGAGAACA-3', reverse primer 5'-TTAGACCGTCCCCATAGTATCCTC-3', probe 5'-FAM-ACATGAAGGTCAATCGAGCCCTACAGGAGAG-TAMRA-3'. *GAPDH* primers and probes for control were purchased from Applied Biosystems. Quantitative real-time PCR analysis was performed by ABI7700 Prism sequence detector (Applied Biosystems), according to manufacturer's instructions using 1 \times TaqMan Universal PCR Master Mix.

After denaturing at 95°C for 10 min, PCR amplification followed by 40 cycles of denaturation at 95°C for 15 s and annealing/extension at 60°C for 1 min. A quantification of *BMCC1* mRNA in each samples was carried out by comparing with a standard curve, which was generated by reacting the plasmid containing *BMCC1*. Furthermore, *GAPDH* mRNA quantification was also performed for a standardization of the initial RNA content of each samples.

Exon prediction and bioinformatics

BLAST search against genome database revealed that 5'-region of *Nbla00219* was matched to the genome sequence of a

BAC clone RP11-146P9 (GenBank accession no. AL161625). We used GENESCAN algorithm (Burge and Karlin, 1997, 1998), and FGENESH algorithm (Solovyev and Salamov, 1999) to predict ORF from the genome sequence, and designed primers from each deduced exons. Using these primers and primers from 5'-region of *Nbla00219* cDNA, RT-PCR was performed to confirm the real exons. All PCR products were sequenced by the ABI automatic DNA sequencer (Perkin-Elmer Cetus) and resulting sequence were assembled to the full-length *BMCCI* cDNA. Bioinformatic analysis was performed using the PSORTII algorithm (Horton and Nakai, 1996), the SOPM algorithm and the TM pred algorithm against the predicted amino-acid sequences of *BMCCI*.

In situ hybridization

Section *in situ* hybridization was carried out as described previously (Takahara *et al.*, 1997). The embryos were collected from pregnant females, and the morning the vaginal plug was detected was recorded as E0.5. A riboprobe was synthesized with digoxigenin-UTP and T3 or T7 polymerase (Roche Molecular Biochemicals). The alkaline phosphatase reaction was performed with NBT-BCIP (Roche Molecular Biochemicals). The riboprobes used for the section *in situ* hybridization were transcripts of the genomic DNA fragments of the *BMCCI* gene, a 835 bp PCR product of exon 3: the primers used are 5'-GAGATACTGGAGTTAGAAGAAG-3' and 5'-TTCGGTCTTGGCTTCTGGGTC-3'.

Immunohistochemistry

NBLs of favorable histology (Shimada system) without *MYCN* amplification and those of unfavorable histology with *MYCN* amplification were analysed. Anti-*BMCCI* antibody was diluted to 1:50 and applied to the immunostaining. After deparaffinization, the sections were treated with 0.05% pronase solution for 5 min at room temperature. The biotin-streptavidin method (Nichirei, Tokyo, Japan) was performed, and the reaction was visualized with diaminobenzidine solution.

Generation of BMCCI transgenic mice

The full-length cDNA encoding human *BMCCI* was subcloned into the *EcoRI* site of the multicloning site region of the transgenic expression vector pCAGGS. The resulting plasmid, pCAGGS-*BMCCI*, was digested by *Alw44I* to isolate the transgenic cassette consisting of the CMV enhancer, the chicken β -actin promoter, the *BMCCI* cDNA, and the rabbit β -globin poly(A) sequence. The isolated region was purified for pronuclear injection into mouse embryos from FVB mice (Charles River Japan Inc.). Mouse embryos (fertilized one-cell zygotes) were injected and implanted in female CD-1 mice (Charles River Japan Inc.) at Japan SLC Inc. (Shizuoka, Japan). *BMCCI* transgenic mice were identified by slot blot analysis using genomic DNA prepared from mouse tails. *BMCCI*-positive founder transgenic mice then were backcrossed at least three times with C57BL/6 mice. Positive mice comprising the F₄ generation were subjected to SCG analyses.

Primary culture of newborn mice SCG cells

Primary cultures of sympathetic neurons were generated from dissociated SCG of postnatal-day 1 wild-type and transgenic mice as described previously (Lee *et al.*, 1980). The cells were plated onto collagen-coated 24-well dishes at a density of around two ganglia per well and maintained in Modified Eagle's Medium supplemented with 10% heat-inactivated donor serum and 50 ng of mouse NGF per ml.

A mixture of uridine and 5-fluorodeoxyuridine (10 μ M each) was added on the following day to eliminate non-neuronal cells.

Statistical analysis

The Student's *t*-tests were used to explore possible associations between *BMCCI* expression and other factors, such as age. Since the values of the *BMCCI* expression were skewed, a log transformation was used to achieve the normality when using *t*-test and Cox regression. The distinction between high and low levels of *BMCCI* was based on the median value of the real-time PCR data (low, *BMCCI* <0.86 d.u.; high, *BMCCI* \geq 0.86 d.u.), regardless of tumor stage, *MYCN* copy, or survival. Kaplan-Meier survival curves were calculated, and survival distributions were compared using the log-rank test. Cox regression models were used to explore associations between *BMCCI*, age, *MYCN*, MS, origin and survival. Statistical significance was declared if the *P*-value was <0.05. Statistical analysis was performed using Stata 6.0. (Stata Corp. 1998. Stata Statistical Software: Release 6.0 College Station, TX: Stata Corporation).

Acknowledgements

We thank Shigeyuki Furuta, Shiho Hamano, Hiroyuki Inuzuka, Aiko Morohashi for technical assistance, Masayuki Fukumura, Toshihide Kanamori and Mika Kimura for helping full-length cDNA cloning, and Shigeru Sakiyama for encouragement. This work was supported in part by a Grant-in-Aid for the 2nd Term Comprehensive 10-Year Strategy for Cancer Control from the Ministry of Health, Labour and Welfare of Japan (AN), and by Grant-in-Aid for Scientific Research (B) (AN) and for Scientific Research on Priority Areas (2) 'Medical Genome Science' (MO, EI, AN) from the Ministry of Education, Culture, Sports, Science and Technology of Japan, and by a fund from Hisamitsu Pharmaceutical Co. Inc. (AN). We also thank following hospitals and departments for providing surgical samples: First Department of Surgery, Hokkaido University School of Medicine; Department of Pediatrics, National Sapporo Hospital; Department of Pediatric Surgery, Tohoku University School of Medicine; Department of Surgery, Gunma Children's Medical Center; Department of Pediatrics, Pediatric Surgery and General Surgery, Jichi Medical University; Department of Hematology and Oncology, Saitama Children's Medical Center; Department of Pediatrics, Juntendo University School of Medicine; Department of Surgery, Kiyose Metropolitan Children's Hospital; Department of Surgery and Pathology, Chiba Children's Hospital; Department of Pediatric Surgery, Chiba University School of Medicine; Department of Pediatric Surgery, Kimitsu Central Hospital; Department of Pediatric Surgery, Niigata University School of Medicine; Department of Pediatrics and Pediatric Surgery, Aichi Medical University; Department of Pediatrics, Kyoto Prefectural Medical University; Tumor Board, Hyogo Children's Hospital; Department of Pediatrics and Pediatric Surgery, Kagoshima University School of Medicine; Department of Pediatric Surgery, Showa University School of Medicine; Department of Pediatrics, Oita University School of Medicine; Department of Pediatric Surgery, Ohta General Hospital; Department of Pediatrics, Ichinomiya City Hospital; Department of Pediatric Surgery, Osaka City General Hospital; Department of Pediatrics, Nihon University School of Medicine Itabashi Hospital; Department of Pediatric Surgery, University of Tsukuba School of Medicine.